第64卷 第3期
2026年7月

古 脊 椎 动 物 学 报
VERTEBRATA PALASIATICA

pp. 254–293
figs. 1–7

DOI: 10.19615/j.cnki.2096-9899.260210
CSTR: 32090.14.j.cnki.2096-9899.260210

Early Pleistocene mammals from Yeka locality in Shangri-La, northwestern Yunnan

ZHANG Li-Min[1,4] CHANG Mei-Jing[1,4] LU Dan[1,4] GONG Hao[1,4] QIN Chao[1,4]
GAO Feng[2] PAN Gao-Yuan[3] LI Gang[3] DENG Tao[1,4] SHI Jing-Song[5]
NI Xi-Jun[1,4*] LI Qiang[1,4*]

(1 *Key Laboratory of Vertebrate Evolution and Human Origins*, *Institute of Vertebrate Paleontology and Paleoanthropology*, *Chinese Academy of Sciences* Beijing 100044)
(2 *Yunnan Institute of Cultural Relics and Archaeology* Kunming 650118)
(3 *Yunnan Diqing Tibetan Autonomous Prefecture Institute of Cultural Administration* Shangri-La 674400)
(4 *University of Chinese Academy of Sciences* Beijing 100049)
(5 *Institute of Zoology*, *Chinese Academy of Sciences* Beijing 100101)
* Corresponding authors: nixijun@ivpp.ac.cn; liqiang@ivpp.ac.cn

Abstract The Early Pleistocene Yeka Fauna was first identified during the Hengduan Mountains Scientific Expedition in the 1980s. New mammal fossil remains were collected during the execution of the Second Tibetan Plateau Scientific Expedition and Research Project (STEP) in 2020 and 2024. The most recent findings have been identified as 5 orders, 12 families, 15 genera, and 15 species. The updated Shangri-La fossil mammal combination (Yeka and Zhongdian faunas) has been compared to several Early Pleistocene faunas in China. It has been found to be most closely correlated to the Yuanmou Man Fauna. The faunal composition of the Shangri-La fossil mammal combination is distinguished by the co-occurrence of boreal and austral elements, a pattern that is analogous to the modern biogeography observed in the Hengduan Mountains. Faunal analysis suggests that during the Early Pleistocene, the Shangri-La region was characterized by a moderate-elevation forest intermingled with open grassland.

Key words Shangri-La, Early Pleistocene, Yeka Fauna, Hengduan Mountains, Paleoenvironment

Citation Zhang L M, Chang M J, Lu D et al., 2026. Early Pleistocene mammals from Yeka locality in Shangri-La, northwestern Yunnan. Vertebrata PalAsiatica, 64(3): 254–293

1 Introduction

The Hengduan Mountain region represents a crucial area for scientific inquiry, encompassing research on biodiversity, biogeography, the Cenozoic uplift of the Tibetan Plateau, and other important topics. The topography of the Hengduan Mountain region in

国家重点研发计划(编号：2023YFF0804500)、国家自然科学基金重点项目(批准号：42430207)、第二次青藏高原综合考察与研究项目(编号：2019QZKK0705)和中国科学院战略性先导科技专项(B类) (编号：XDB26030300)资助。
收稿日期：2025-03-28
©The Author(s) 2026. This is an open access article under the CC BY-NC-ND License.

the southwest of China is diverse, and the region is home to an exceptionally rich array of biological resources (CSEQXP of CAS, 1983, 1986; Zhang et al., 1997; Zhao and Yang, 1997). The Hengduan Mountains are recognized as one of the 25 global biodiversity hotspots, which exhibit the highest levels of biodiversity on Earth (Boufford and van Dyck, 2000; Myers et al., 2000; Mittermeier et al., 2005, 2011). One study hypothesizes that the formation of the modern high biodiversity in the Hengduan Mountains was driven by the uplift of the Tibetan Plateau during the Late Miocene, approximately 8 Ma (Xing and Ree, 2017). However, recent studies suggest that the high biodiversity observed in the Hengduan Mountains was already established as early as the Early Oligocene, approximately 30 to 34 Ma (Ding et al., 2020; He et al., 2022). The Hengduan Mountains region is located in the transition zone between the Oriental and Palearctic regions (Chen et al., 2008; Zhang et al., 2009a). It is the original center of numerous modern endemic species (Zhang et al., 2009b; Huang et al., 2016; Du et al., 2017; Ge et al., 2021; Wang K et al., 2022; Wang X et al., 2022; Chen et al., 2023) and serves as a refuge for some relict species, allowing them to adapt to the Quaternary glacial periods (Li et al., 2012; Yu et al., 2013; He and Jiang, 2014; Meng et al., 2015; Li et al., 2023; Liu L P et al., 2023). The formation of the Hengduan Mountains and its high biodiversity are attributed to the Cenozoic southeastward extrusion of the southeastern Tibetan Plateau in response to the Indian-Eurasian collision and climate change (Tapponnier et al., 1982; Sun et al., 2017; Mao et al., 2021). The analysis of the Cenozoic basins and their fossils can provide evidence for reconstructing the uplift process of the southeastern Tibetan Plateau and elucidate the evolution of biodiversity and biogeography in the Hengduan Mountain region.

From 1982 to 1985, a team of vertebrate scientists, organized by the Institute of Vertebrate Paleontology and Paleoanthropology, Chinese Academy of Sciences (IVPP), conducted an investigation of the Hengduan Mountain region with the objective of locating Cenozoic deposits and their associated vertebrate fossils. This investigation was a continuation of the First Tibetan Plateau Scientific Expedition (1973–1979). The investigation in the Hengduan Mountains yielded the discovery of over forty valuable mammalian fossil localities spanning the Middle Eocene to the Pleistocene (Zong, 1987a, b; Zong et al., 1996). One of the Pleistocene localities discovered in this investigation is Yeka, Nixi in Zhongdian (now renamed Shangri-La). During the course of the Second Tibetan Plateau Scientific Expedition and Research Project (STEP, http://www.step.ac.cn/), a new team from the IVPP relocated the Yeka locality, collected a substantial quantity of matrix, and conducted wet-sieving in 2020 and 2024. The present paper sets out to describe the novel findings of this project.

2 Geographical and geologic settings

The Yeka fossil site (28°05′02.61″N, 99°28′54.07″E) is located in the Nangou area of Yeka Village, Nixi Township, ~35 km northwest of Shangri-La city (formerly Zhongdian),

Yunnan Province (Fig. 1). The contemporary climate classification for the Shangri-La region is that of a temperate and cold temperate monsoon climate, while the river valley area is classified as a northern subtropical monsoon climate. The annual average temperature (AAT) is recorded at 6.3°C, while the annual average precipitation (AAP) is 651.1 mm. The predominant vegetation comprises coniferous forests, broadleaf forests, alpine shrubs, and alpine meadows, which exhibit typical vertical zonation characteristics (Li et al., 2022).



Fig. 1 The location of the Yeka Fauna and related Early Pleistocene Faunas in China

The Shangri-La region has seen the development of three minor intermontane faulted basins: the Nixi Basin, the Zhongdian Basin, and the Xiaozhongdian Basin (Cheng, 1994). The Yeka fossil site is located within the Nixi Basin, while the Zhongdian Fauna, an assemblage of Early Pleistocene fossils, was recovered from the Zhongdian Basin (Ma et al., 2004). The tectonic activity in these basins is influenced by the Deqin-Zhongdian-Daju Fault (Chang et al., 2014; Liu et al., 2023). The late Cenozoic deposits are preserved in these basins with varying thickness. Of the exposed deposits that are currently observable, the oldest is a series of lacustrine and paludal deposits comprising marlstones, mudstones, silt mudstones, and gravels interbedded with laminated lignite. The thickness of this sedimentary succession is estimated to be about 250–300 m. Palynological analysis of the sediments has revealed that the spore pollens obtained from the strata are predominantly of the broad-leaved *Quercus*, *Betula*, and *Ulmus*. It is widely regarded as being contemporaneous with the Sanying Formation and as dating from the Late Pliocene (Zhang et al., 1996; Wang et al., 1999). The lower Pleistocene

deposits are preserved in the Nixi and Zhongdian basins. In the Nixi Basin, the lower Pleistocene deposits yielded the Yeka Fauna and are unconformably overlain on underlying Pliocene lignite-bearing sediments. In the Zhongdian Basin, the lower Pleistocene deposits are composed of Grayish-white silty clay, intercalated with yellow silty clay lenses, which yielded the Zhongdian Fauna (Ma et al., 2004). On the other hand, the upper Pleistocene deposits are primarily concentrated in the Xiaozhongdian Basin and consist of a series of lacustrine clays, silt clays, sands, and gravels (Zhao et al., 2007). The Xiaozhongdian Basin has been found to contain a significant number of paleolithic artifacts (Gao et al., 2024).

The Yeka fossil site is located in a tributary gully on the eastern bank of the Jinsha River. The fossil-bearing beds directly overlie a Pliocene lacustrine coal-bearing bed, reaching a thickness of about 50 m and an elevation of about 3750 m. The fossil-bearing beds consist of fluvial facies deposits and can be divided into two parts: an upper and a lower part. The lower part consists of a brown gravel and sandy clay layer with relatively robust cementation, while the upper part is characterized by brownish-red clay with abundant calcareous nodules and mammalian fossils. This upper layer is further capped by brownish-red slope remnants, including breccia and clay. It is noteworthy that prior to the deposition of these fossil-bearing strata, significant neotectonic activity occurred, resulting in pronounced folds and faults in the underlying coal-bearing strata (Zong, 1987a; Zong et al., 1996).

3 Material and methods

A total of 4.5 tons of matrix were collected from four sites (NXYK01, 02, 03, and 04) of the Yeka locality in 2020. The matrix was subsequently transported to the IVPP workstation in Qujing, Yunnan, where it underwent a thorough washing process. Sixteen mammal specimens were obtained through the wet-sieving technique (Li and Ni, 2021). Additionally, other large mammal remains were collected during the fieldwork seasons of 2020 and 2024. The observation and measurement of small mammals was conducted under an OLYMPUS SZX7 microscope with a precision of 0.01 mm. The specimens were then scanned by a Micro CT instrument (160 kV) in the High-Resolution X-ray Computed Tomography Laboratory, IVPP, and 3D imaging was performed by using VG Studio 3.4 (legitimate).

The terminology employed for the Lagomorpha p3 in this text is based on White (1991), while the terminology for the Arvicolidae molars is derived from Zheng (2020). The terminology for the Cricetidae molars follows Wang et al. (2020), that of the Muridae molars follows Chang et al. (2023), that for the Ruminantia (Cervidae, Bovidae) cheek teeth follows Bärmann and Rössner (2011), that of the Viverridae cheek teeth follows Zack (2012), and that of the Equidae cheek teeth follows Eisenmann et al. (1988), respectively.

Institutional abbreviations C, specimens bear designations of the earlier Cenozoic Laboratory of the Geological Survey of China; HV, field locality number of Hengduan

Mountain region; IVPP, Institute of Vertebrate Paleontology and Paleoanthropology, Chinese Academy of Sciences, Beijing, China; RV, revised specimen number, replacing numbers formerly used in IVPP; THP, prefix for specimen numbers of the Tianjin Natural History Museum; V, CP, prefix of vertebrate fossils stored in IVPP; YS, field locality number of Yushe Site.

4 Systematic paleontology

Order Lagomorpha Brandt, 1855

Family Ochotonidae Thomas, 1897

Genus *Ochotonoides* Teilhard de Chardin & Young, 1931

***Ochotonoides complicidens* (Boule & Teilhard de Chardin, 1928)**

(Fig. 2A–C)

Referred specimens Three specimens: an isolated left dp3 from NXYK03, IVPP V34068.1; a right fragmentary mandible with p3–4 from NXYK01; and a right fragmentary mandible with m2–3 from NXYK03, V34068.2.

Measurements (in mm) The length×width: dp3: 2.3×1.7, m2: 2.05×2.04, m3: 0.95×1.8. For other measurements, see Table 1.

Description The two mandibles are fractured. The V34068.2 preserves only a portion of the horizontal ramus of the dentary and p3–4. In contrast, V34068.3 retains the base of the ascending ramus and the posterior region of the horizontal ramus with m2–3. On the buccal side of V34068.1, multiple nutrition foramina are present beneath the premolars. Its p3 exhibits a trapezoidal occlusal contour. The anterior lobe is oriented in an anterobuccal direction. The p3 comprises four reentrants, including the anterior reentrant (AR), the anteroexternal reentrant (AER), the posteroexternal reentrant (PER), and the anterointernal reentrant (AIR).

Table 1 Measurement comparison among different specimens of *Ochotonoides* (mm)

Locality	Reference	Inventory number	Species	Dentary height at p4	p3 length×width
Yeka	This text	V34068.1	*O. complicidens*	9.00	2.20×2.00
Majuangou	Cai et al., 2008	V15270.1	*O. complicidens*		2.25×2.00
		V15270.2			2.50×2.30
Heshui	Wu and Flynn, 2017a	V4776	*O. complicidens*		2.25×2.05
Baihai		THP14190	*O. complicidens*	12.40	2.74×2.40
Qingyang(type)		THP25.918	*O. complicidens*		2.60×2.65
Gaozhuang		THP14242	*O. complicidens*	13.20	2.93×2.25
Loc. 18 of Zhoukoudian/ (Huiyu)		CP 110	*O. complicidens*	10.80	2.60×2.39
Chenjiawo		V3155	*O. complicidens*	11.80	2.90×2.60
Yulin		C/100	*O. complicidens*	11.90	3.00×2.70
Malan		THP14208	*O. teilhardi*	10.30	2.30×2.15
Baihai		THP14191	*O. teilhardi*		2.35×2.05
YS5		V11200.1	*O. teilhardi*	9.80	2.35×2.25
YS99		V11202.1	*O. teilhardi*	10.30	2.35×2.27
YS6		V11204.1	*O. teilhardi*		2.30×2.15

The posterointernal reentrant (PIR) is absent. The AR is longitudinally deep into the occlusal surface. The transverse AER and oblique AIR are arranged in an alternating pattern, and the enamel bridge between the two reentrants is notably narrow. Additionally, the PER is oblique. The lingual wall of the posterior lobe is observed to be straight. The enamel thickness is heterogeneous. All the reentrants are filled with cement.

The dp3 comprises three lobes, which gradually widen from the anterior to posterior. The tooth is characterized by the presence of two anterior and two posterior folds. The former is shallow and devoid of cements, while the latter deeply extends into the occlusal facet and is filled with cements. The tooth is moderately crowned.

The p3 exhibits a subtriangular occlusal outline. The AR (=anteroflexid) is relatively well-developed and extends posteriorly. The AER (=protoflexid) and the AIR (=paraflexid) are situated in opposition to one another and oriented posteriorly oblique. They are fully filled with cement. The enamel bridge is central and notable for its narrowness. Two small plications are present on the anterior wall of the AIR. The PER (=hypoflexid) does not reach the half-width and is posteriorly oblique. The PIR (=metaflexid) is not developed.

The p4 and m2 exhibit a comparable structure, comprising an anterior lobe and a posterior lobe. No enamel connection exists between the two lobes. Both lobes are anteroposteriorly compressed, with the anterior lobe exhibiting a higher elevation than the posterior lobe.

The m3 has a single lobe, with a posteriorly curved base portion.

Remarks The three specimens provide evidence of a large ochotonid from the Yeka locality. In light of the relatively large dimensions of the teeth and the intricate occlusal pattern of the p3, the three specimens from Yeka can be attributed to the genus *Ochotonoides*. This genus is known as an endemic genus discovered in the Pliocene to Pleistocene of China (Zhang, 2019), and comprises three species: *O. complicidens*, *O. bohlini*, and *O. teilhardi* (Boule and Teilhard de Chardin, 1928; Erbajeva, 1988; Wu and Flynn, 2017a). *O. bohlini* is distinguished from the other species by the development of two deep anterior reentrants in the anterior lobe of the p3. In contrast, *O. teilhardi* exhibits a reduced but distinct shallow groove (lingual anterior reentrant) at the anterior lobe of the p3. The absence of a lingual anterior reentrant in the anterior lobe of the p3 in the Yeka material indicate that it can be attributed to *O. complicidens* rather than to *O. bohlini* or *O. teilhardi*. *O. complicidens* was primarily identified from the Late Pliocene to the Early Pleistocene in northern and central China, including Qingyang (Boule and Teilhard de Chardin, 1928), Heshui (Zheng, 1976), and Lingtai (Zheng and Zhang, 2000, 2001) in Gansu, Jingle (Teilhard de Chardin and Young, 1931) in Shanxi, Lantian (Chow and Li, 1965; Ji, 1976; Hu and Qi, 1978) and Yulin (Teilhard de Chardin and Young, 1931) in Shaanxi, the Nihewan Basin (Teilhard de Chardin and Piveteau, 1930; Cai et al., 2008) in Hebei, Huiyu (Locality 18 of Zhoukoudian) (Teilhard de Chardin, 1940) in Beijing, Dalian (Jin et al., 2021) in Liaoning , and Yunxian (Liu and Zheng, 1997) in Hubei.

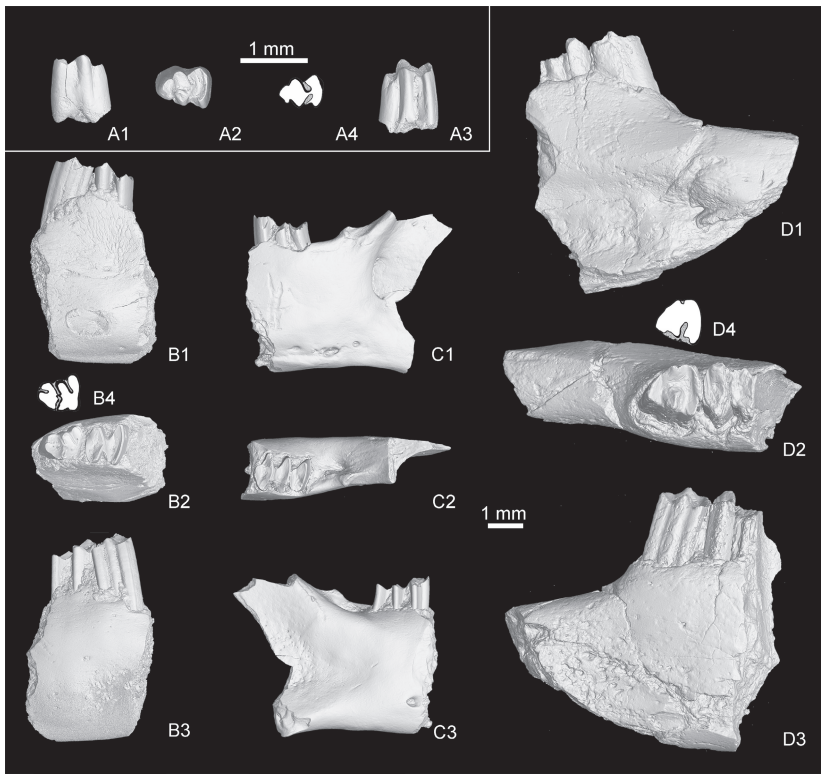


Fig. 2 Lagomorpha remains from Yeka locality, Shangri-La, Yunnan
A–C. *Ochotonoides complicidens*: A. IVPP V34068.1, left dp3;
B. V34068.2, right fragmentary mandible with p3–4; C. V34068.3, right fragmentary mandible with m2–3;
D. *Hypolagus* cf. *H. schreuderi*, V34069, left fragmentary mandible with p3–4
A1–D1. lingual views; A2–D2. occlusal views; A3–D3. buccal views;
A4, B4, D4. line drawings of p3, respectively

Family Leporidae Gray, 1921

Genus *Hypolagus* Dice, 1917

***Hypolagus* cf. *H. schreuderi* Teilhard de Chardin, 1940**

(Fig. 2D)

Referred specimen A left fragmentary mandible with p3–4 from NXYK02, IVPP V34069.

Measurements (in mm) Dentary height beneath p4, ~12.0; occlusal length×width: p3: 3.0×3.0, p4: 3.0×3.0. For other measurements, see Table 2.

Description The anterior part and the posterior horizontal (angular and condyloid) and ascending rami are damaged. Only a portion of the horizontal ramus bearing the diastema, the posterior part of the lower incisor, and the p3–4 preserved. In the buccal view, the posterior half of the mental foramen is visible on the buccal side of the diastema, situated horizontally at a distance of about 4.5 mm anterior to the anterior margin of the p3. The incisor does not exhibit any outward bulging. Multiple nutrition foramina are evident in the region posterior to

the mental foramen. In the lingual view, a distinct pit is observed that is vertical to the anterior margin of the p3, which may be the fossa digastrica.

The p3 exhibits a triangular occlusal contour. In the buccal view, a cement-filled AER (=protoflexid) and PER (=hypoflexid) are evident. The former is markedly transversely shallow, while the latter traverses nearly half the occlusal surface. The two flexids persist far down the shaft. In the lingual view, there is a very shallow PIR.

The p4 has two lobes. The anterior lobe is connected to the posterior lobe by a thin lingual enamel bridge. The anterior lobe is wider and higher than the posterior lobe.

Remarks The p3 of this Yeka material exhibits a typical occlusal pattern of *Hypolagus*, characterized by the absence of a lingual anterior reentrant, the reduction of the lingual posterior reentrant, the presence of only two buccal folds, and the absence of an AR in the anterior lobe. The genus *Hypolagus* is widely distributed throughout the northern hemisphere from the Pliocene to the Middle Pleistocene (Kurtén, 1968; McKenna and Bell, 1997; Quintana et al., 2010; Li, 2019). It is noteworthy that two previously referred species, *H. brachypus* from Huiyu, Beijing (Young, 1927) and *H. sivalensis* from the Upper Siwaliks of Pinjor, India (Forsyth Major, 1899), have already been transferred to *Sericolagus* and *Pliosiwalagus*, respectively (Averianov, 1996; Patnaik, 2001, 2002). The p3 of the Yeka material exhibits a distinct morphological divergence from the two aforementioned species.

The Chinese *Hypolagus* is known to comprise three species: *H. mazegouensis*, *H. fanchangensis*, and *H. schreuderi* (Teilhard de Chardin, 1940; Jin and Xu, 2009; Wu and Flynn, 2017a). Distinguishing between these species is facilitated by the position of the posterior end of the lower incisor relative to the p3 (Li, 2019). We conducted computed tomography (CT) scanning to observe the position of the posterior end of the lower incisors of *H. mazegouensis* (IVPP V11224.2) from the late Pliocene of the Yushe Basin, Shanxi. Additionally, the specimens V13977.1 of *H. fanchangensis* and RV42011.25 of *H. schreuderi*, which were collected from the Early Pleistocene deposits of Fanchang, Anhui, and the Early Pleistocene Huiyu (Locality 18 of Zhoukoudian), Zhoukoudian, Beijing, respectively, and the Yeka specimen (V34069), were also analyzed (Fig. 3). The results demonstrate that the lower incisors of *H. mazegouensis* and *H. schreuderi* terminate posteriorly at the buccal side of the anterior wall of the p3 (Fig. 3B,C), while that of *H. fanchangensis* terminates posteriorly at

Table 2 Measurement comparison among different species of *Hypolagus* (mm)

Locality	Reference	Inventory number	Species	Dentary height at p4	Dentary height at m1	Width of p3	Length of p3–4
Loc. 18 of Zhoukoudian	This text	RV42011.25	*H. schreuderi*	15.1	15.1	3.5	6.7
YS5	This text	V11224.2 (juvenile)	*H. mazegouensis*	12	12		
Fanchang	This text	V13977.1 (Type)	*H. fanchangensis*	13.4	13.3	3.0	5.8
Wangbuding	Zong et al., 1996	HV7708	*H.* cf. *H. schreuderi*		13.5	3.2	6.2
Yeka	This text	V34069	*H.* cf. *H. schreuderi*	12.1		3.0	6.0

the buccal side of the p4 (Fig. 3D). The lower incisor of the Yeka specimen terminates at the buccocentral side of the p3 (Fig. 3A). The specimen of *H.* cf. *H. schreuderi* from the Early Pleistocene of Wangbuding, Dege, Sichuan, is currently unavailable. As outlined by Zong et al. (1996), the lower incisor of *H.* cf. *H. schreuderi* is observed to terminate posteriorly at the anterior wall of the p3. In comparison to *H. schreuderi*, the Yeka specimen's dentary height beneath the p4 is lower and the cheek teeth are proportionately smaller. In comparison to *H. fanchangensis*, the Yeka specimen exhibits a shorter height beneath the p4 and the lower incisor extends more shallowly posteriorly. In comparison to *H. mazegouensis*, the lower incisor of the Yeka specimen extends more deeply posteriorly. The Yeka specimen is most similar to *H.* cf. *H. schreuderi* from Wangbuding, and they both may represent a new species that occurred in the eastern region of the Tibetan Plateau.

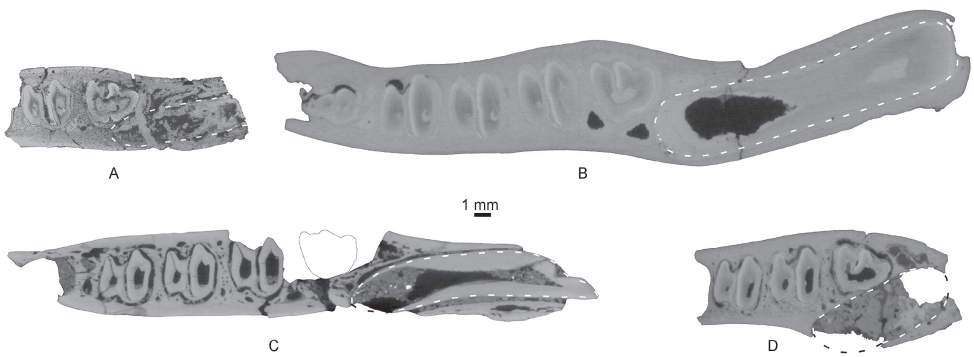


Fig. 3 CT slices of *Hypolagus* mandibles show the position of the lower incisor termination
A. *Hypolagus* cf. *H. schreuderi*, IVPP V34069; B. *H. schreuderi*, RV42011.25 (reversed); C. *H. mazegouensis*, V11224.2 (reversed); D. *H. fanchangensis*, V13977.1

Order Rodentia

Family Arvicolidae Gray, 1821

Tribe Lagurini Kretzoi, 1955

Genus *Mimomys* Forsyth Major, 1902

***Mimomys* (*Cromeromys*) *gansunicus* Zheng, 1976**

(Fig. 4A–C)

Referred specimens Three specimens: a left M1 from NXYK03, IVPP V34061.1; a right M2 from NXYK04, V34061.2; a right m1 from NXYK01, V34061.3.

Measurements (in mm) Maximum length×maximum width, M1: 2.65×1.60; M2: 1.5×1.15; m1: 2.5×1.25.

Description The molars are filled with cement and have roots.

The M1 comprises three lingual salient angles (LSA) and three buccal salient angles (BSA). The anterior wall of the tooth exhibits a slight convexity. The inner corners of the reentrant angles exhibit a slight posterior curvature. Isthmuses 1 and 3 are nearly sealed, while

isthmuses 2 and 4 are wide. The posterior aspect of the tooth is notably protruding. The enamel is disrupted in the external corners of the anterior loop, the triangle 1 (or the protocone), and the posterior wall of the posterior loop. In lateral view, the dentine tract is peaked at the lateral sides of the buccal salient angle of the anterior loop, the lingual salient angles of the anterior loop and the triangle 1 (or the protocone), and the posterior wall of the tooth.

The M2 exhibits a comparable occlusal morphology to that of the M1, with the exception of the absence of the lingual portion of the anterior loop. The two lingual salient angles are more quadrate than the three buccal salient angles. In the occlusal view, the enamel is continuous without any disruption. In the lateral view, the dentine tract undulates at each prism. The peaks at the lateral side of the BSA3 and the LSA2 are the highest. The M2 has two roots.

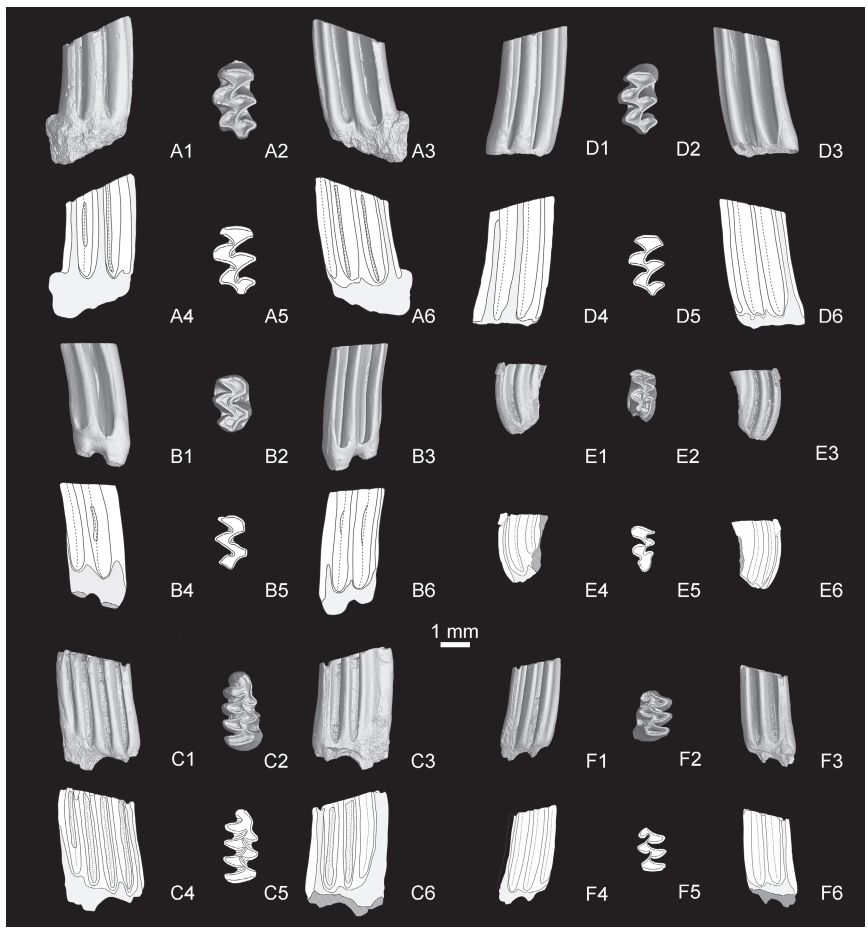


Fig. 4 Arvicolidae molars from Yeka, Shangri-La, Yunnan
A–C. *Mimomys* (*Cromeromys*) *gansunicus*: A. left M1, IVPP V34061.1, B. right M2, V34061.2, C. right m1, V34061.3; D–F. *Villanyia hengduanshanensis*: D. left M1, V34062.1, E. right M3, V34062.2, F. left m2, V34062.3
A1–F1. lingual views; A2–F2. occlusal views; A3–F3. buccal views; A4–F4. line drawings of lingual; A5–F5. line drawings of occlusal; A6–F6. line drawings of buccal respectively

The m1 is constituted by five triangles located between the anterior cap and the posterior loop. The contour of the anterior cap is relatively simple and exhibits an elliptical shape oriented anterolingual-posterobuccally. The anterior loop is devoid of an enamel island. The *Mimomys* ridge (MR) is not present. The lingual reentrant angle 4 (LRA4) and the buccal reentrant angle (BRA3= islet fold, IF) are less deep in the occlusal surface than the other posterior lingual and buccal re-entrant angles, respectively. Isthmus 5, which is located between the anterior cap and the triangle (T5), is broad, while the other posterior isthmuses (1–4) are closed. In the occlusal view, the enamel is disrupted at the anterior wall and the lateral corners of the posterior loop. In the lateral view, the dentine tract is peaked at the anterior wall and the external corners of the posterior loop, and the islet fold extends to the tooth base. The dentine tract indices of E, Ea, Eb, and HH are 3.0, 2.8, 2.8, and 4.3 mm, respectively. The SDQ is greater than 100%.

Remarks These three specimens differ from those of *Villanyia hengduanshanensis* from the Yeka locality in the presence of cements and by having a larger SDQ value. Furthermore, the m1 is devoid of *Mimomys* ridge, and the M2 possesses two roots. These characteristics align with the diagnosis of *Mimomys* (*Cromeromys*) *gansunicus*, as amended by Zheng (2020). *M.* (*C.*) *gansunicus* is an extinct arvicolid species discovered in the Late Pliocene to the Early Pleistocene period in northern and central China.

Genus *Villanyia* Kretzoi, 1956

***Villanyia hengduanshanensis* (Zong, 1987)**

(Fig. 4D–F)

Referred specimens A left M1 from NXYK03, IVPP V34062.1; a right M3 and a left m2 from NXYK01, V34062.2, V34062.3.

Measurements (in mm) M1: 2.45×1.40; M3: 0.9×0.7; m2: 2.30×1.80.

Description The molars are devoid of any cement fillings and have roots.

The M1 occlusal pattern is formed by the anterior cap (AC) and the four posterior triangles. The tooth exhibits three lingual and two buccal reentrant angles. The anterior wall of the anterior cap is straight. The buccal corner of the anterior cap is curved. The isthmuses are narrow in width but not sealed. The dentine tract (DT) is sharp and extends almost to the occlusal facet along the lingual corner of the anterior cap and the triangle 1 (=protocone), while it is undeveloped at the triangle 3 (=hypocone). The crown height is 4.2 mm, while the heights of the anterosinulus (Asl), the prtosinus (Prs), the hyposinuid (Hys), and distosinus (Ds) are 3.8, 4.2, 0, and 4.2 mm, respectively. Additionally, the buccal dentine tract exhibits undulation. The heights of the anterosinus (As), the parasinus (Pas), and the metasinus (Mes) are 4.2, 0.5, and 0 mm, respectively.

The M3 exhibits slight fracturing. The anterior and posterior loops are devoid of enamel islands. The lingual anterior wall of the anterior loop exhibits a slight convexity. The buccal

side exhibits three BSAs and two BRAs, while the lingual side displays two LSAs and two LRAs. The anterior wall of the BRA1 is vertical to that of the LRA2. The LSA2 is more rounded in shape and less acute than the BSA1. The BSA2 is relatively delicate in comparison to the other angles. The LRA2 and the BRA2 extend lingually into the central portion of the crown, curving in a manner reminiscent of an eagle's beak and extending posterolaterally. The isthmus between the T2 and the T3 is narrow. The Is4 is open and the T3 is not confluent with the posterior loop. The LSA3 is well developed, while the LRA3 is shallow. The BSA3 is inconspicuous. In lateral view, the DT is observed to be peaked at the lateral sides of the LSA2 and the BSA1, extending to the occlusal surface. Conversely, the dentine tract is observed to be low at the base of the lateral sides of the posterior angles. The SDQ is less than 100%.

The m2 exhibits three BSAs, two LSAs, two BRAs, and two LRAs. The triangles are alternately arranged. The isthmus is almost sealed. Additionally, the anteroconid lacks the anterior convexity. The enamel of the anterior wall is disrupted by the presence of a peaked dentine tract. In lateral view, the DT is observed to be peaked at the lateral sides of the BSA1 and LSA1, extending to the occlusal surface. Conversely, the dentine tract is observed to be low at the base of the lateral sides of the anterior angles.

Remarks These three teeth are characterized by the absence of cementum, the presence of roots, and the short and wide posterior loop of the M3. The size and morphology of the m2 are identical to those of *Villanyia hengduanshanensis* from the Yeka and Wangbuding localities, which were originally referred to the genus *Mimomys* (Zong, 1987a; Zong et al., 1996) and subsequently transferred to the genus *Villanyia* (Qiu and Li, 2016; Zheng, 2020). We propose that these teeth be classified as *V. hengduanshanensis*.

Family Rhizomyidae Miller & Gidley, 1918

Subfamily Rhizomyinae Miller & Gidley, 1918

Genus *Rhizomys* Gray, 1831

***Rhizomys pruinosus* Blyth, 1851**

(Fig. 5)

Referred specimens Four specimens from NXYK02, including two m1s and two M3s, V34063.1–4.

Measurements (in mm) Maximum length×maximum width, occlusal, m1s: 4.3×3.0, 4.2×2.8; M3s: 4.0×3.2, 3.7×3.7.

Description The upper molars are unilaterally high-crowned with the lingual surface exhibiting a notably higher level of development than the buccal surface. The occlusal surface of the M1 exhibits a rectangular contour, formed by two loops. The anterior loop is constituted by the anteroloph and the protoloph, whereas the posterior loop is formed by the mesoloph and the metaloph-posteroloph complex. The anterior loop is enclosed, while the posterior loop is open buccally. Due to extensive wear, the anterior loop and the posterior loop appear to

be nearly connected by the buccoposterior protuberance of the protoloph at the buccal tooth margin. Three synclines are present on the occlusal surface, including a curved anterior, a deep sinus, and an oblique posterior. In the lateral view, the sinus extends down to the base of the tooth.

Two specimens of M3 have been identified, exhibiting notable differences in wear. One (IVPP V34063.3) is slightly worn and is believed to belong to a younger individual, while another (V34063.4) is heavily worn and is thought to be from an older individual. The occlusal patterns of both specimens are constituted by four transverse ridges, which, from anterior to posterior, are the anteroloph, the protoloph, the mesoloph, and the metaloph-posteroloph complex, respectively. In the V34063.3, the mesoloph is separated from the metaloph-posteroloph complex on the lingual side, whereas in the V34063.4, these structures are connected. The anteroloph and the mesoloph are separated in both specimens. The metaloph-posteroloph complex lacks an enamel islet. A cleavage or convex is present at the middle of the anterior wall of the metaloph-posteroloph complex.

Remarks The presence of the four molars at the Yeka locality provides evidence that a rhizomyid may have existed there. The Yeka material is distinguished by a high crown, a slender M1 that is longer than it is wide, and a notably large-sized M3 in comparison to the M1. The dental morphology of the four molars is identical to that of the genus *Rhizomys*. The fossil materials from the Late Pliocene to the Late Pleistocene of China belonging to the genus *Rhizomys* were identified as *R.* (*Brachyrhizomys*) *shansius*, *R.* (*B.*) *shajius*, *R.* (*Rhizomys*) *sinensis*, *R.* (*R.*) *brachyrhizomysoides*, *R.* (*R.*) *fanchangensis*, *R.* (*R.*) *pruinosus*, *R.* (*R.*)

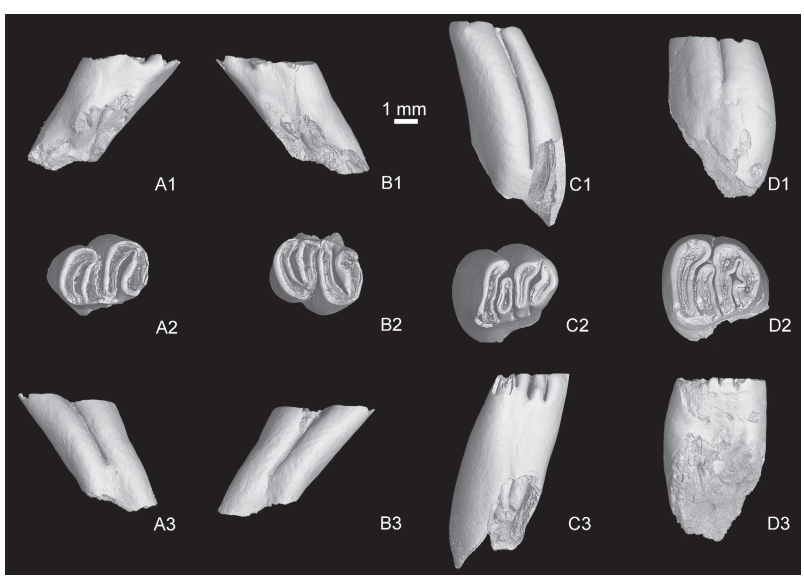


Fig. 5 Molars of *Rhizomys pruinosus* from Yeka, Shangri-La, Yunnan
A. left m1, IVPP V34063.1; B. right m1, V34063.2; C. right M3, V34063.3; D. right M3, V34063.4
A1–D1. lingual views; A2–D2. occlusal views; A3–D3. buccal views

schlosseri, and *R.* (*R.*) *troglodytes* (Qiu, 2020). The Yeka specimens exhibit high crowns that are distinct from the low-crowned subgenus *Brachyrhizomys*. Additionally, the high crown, the size, and the occlusal pattern of the Yeka specimens are also divergent from those of *R. brachyrhizomysoides*, *R. fanchangensis*, *R. schlosseri*, and *R. troglodytes*. *Rhizomys* comprises three extant species: *R. sinensis*, *R. sumatrensis*, and *R. pruinosus*. As identified by López-Antoñanzas et al. (2013), *R. pruinosus* can be distinguished from the other two species by the slender contour of its M1 and the large size of its M3. The four molars are identical to those of *R. pruinosus* in dental morphology, and thus can be classified as this species. *R. pruinosus* is currently distributed in southern China, the Indo-China Peninsula, and northwestern India, and is a typical oriental taxon. It is adapted to bamboo thickets or beardgrass environments with low elevations of less than 1500 m (Norris, 2017). The discovery of *R. pruinosus* in the Yeka locality indicates a rather low elevation during the Early Pleistocene.

Family Cricetidae Fischer von Waldheim, 1817

Subfamily Cricetinae Fischer von Waldheim, 1817

Genus *Cricetinus* Zdansky, 1928

Cricetinus varians Zdansky, 1928

(Fig. 6D, E)

Referred specimens A left M2 from NXYK01, IVPP V34064.1; a left m2 from NXYK03, V34064.2.

Measurements (in mm) Maximum length×maximum width, M2: 1.80×1.50; m2: 1.76×1.40.

Description The M2 has an approximately square occlusal shape. The main cusps are sharp and slightly worn. Both the buccal and lingual branches of the anteroloph are developed. The buccal branch is higher than the lingual branch. The anterolophule is double and short. The lingual anterolophule is attached posteriorly to the anterior arm of the protocone, while the buccal anterolophule posteriorly connects to the anterior protolophule. A small pit is enclosed by the buccal and lingual anterolophules, the anteroloph, and the anterior protolophule. The protolophule is double. The mesocone is absent. The mesoloph is short and attaches to the anterior wall of the metacone. The endoloph is curved. The metalophule I is short and anteriorly connects to the middle of the mesoloph. The metalophule II is absent. The posteroloph is developed and extends to the buccoposterior wall of the metacone. The protosinus is shallow and open, while the parasinus is deep and closed. The metasinus is closed. The posterosinus is absent. The roots are not preserved.

The m2 has a rectangular occlusal contour. The main lingual cusps are more anterior than the opposite buccal cusps. The anterolophid has only one buccal branch. The buccal branch originates from the middle of the anterior wall and extends buccally and downward to the base of the buccoanterior wall of the protoconid. A large protosinusid is present. The metalophid

is short and directed buccoanteriorly. The mesoconid and the mesolophid are absent. The ectolophid is curved. The hypolophid is buccoanteriorly fused with the posterior arm of the protoconid. The posterolophid is developed and slightly posteriorly bugled. The metasinusid is open, and it has two roots.

Remarks The two molars represent the occurrence of a hamster from the Yeka mammalian assemblage. They possess some derived characters, such as the absence of the mesocone and the mesoconid, the endomesoloph and the ectomesolophid, and the lingual branch of the anterolophid, and the reduction of the mesoloph. These characters differ from those of the Neogene hamsters. Their dental pattern is simple and close to that of the extant *Cricetulus*. However, the M2 of Yeka remains a reduced mesoloph. We have placed these two hamster molars in the genus *Cricetinus*. According to the review by Wang et al. (2020), *Cricetinus* has two species, *C. varians* and *C. mesolophidos*. *C. mesolophidos* is a large species and only occurs in the Early Pliocene of the Yushe Basin in Shanxi Province (Wu and Flynn, 2017b). *C. mesolophidos* has primitive characters, such as the presence of a long mesolophid, the lingual branch of the anterolophid, and the posterosinus. *C. varians* is smaller in size than the *C. mesolophidos*, and has derived characters on the molars. It is widely distributed in the Early to Middle Pleistocene of northern and central China (Zdansky, 1928; Zheng, 1984). The Yeka material is attributed to *C. varians* by both its small size and its derived dental characters.

Family Muridae Illiger, 1811

Subfamily Murinae Illiger, 1811

Genus *Micromys* Dehne, 1841

***Micromys minutus* (Pallas, 1771)**

(Fig. 6C)

Referred specimen A left m1 from NXYK01, IVPP V34066.

Measurements (in mm) Maximum length×maximum width, 1.5×0.88.

Description The m1 is low-crowned, long, and narrow anteriorly. The anterocentral cusp (Acc=tma) is distinct and joins the anterolingual cusp (Alc) linguoposteriorly. The Alc is almost equal in size to the anterobuccal cusp (Abc) and slightly anterior to the Abc. The paired anteroconids are connected to the posterior protoconid-metaconid pair by the anterior mure (Am). The Alc, Abc, protoconid, and metaconid form an "X" pattern. The longitudinal spur (Ls) is absent. A deep central chevron cleavage separates the anterior four cusps and the posterior two main cusps. The entoconid is more anterior than the hypoconid. The posterior cingulid (Pcd) is large, triangular shaped, and slightly lingual. A spur is present on the anterior of the Pcd. The posterior c1 is well developed and has a triangular worn facet. Anterior c2 and c3 are inseparable. The buccal stylids form a continuous longitudinal ridge that is lower than the main buccal cusps. The m1 has three roots, including two main roots and a small central root on the buccal side.

Remarks The tooth represents the occurrence of a small-sized murid in the Yeka fossil assemblage. It is small-sized and characterized by the presence of a developed anterocentral cusp and a low continuous buccal cingulid, as well as the absence of the longitudinal spur. Based on the size and dental morphology, this m1 has been assigned to *Micromys minutus*. *M. minutus* is a cosmopolitan species distributed throughout Eurasia from the Early Pleistocene to the present (Wu, 2020).

Genus *Apodemus* Kaup, 1829

Apodemus latronum Thomas, 1911

(Fig. 6B)

Referred specimen A left M1 from NXYK03, IVPP V34065.

Measurements (in mm) Maximum length×maximum width, 2.3×1.42.

Description The M1 has a pear-shaped occlusal contour and is moderately crowned. The anterior portion is slightly narrow. The anterior cingulum, t1bis, and t2bis are absent. Cusp t1 is larger than and posterior to cusps t2 and t3. Cusp t3 is smaller than t2. The posterior

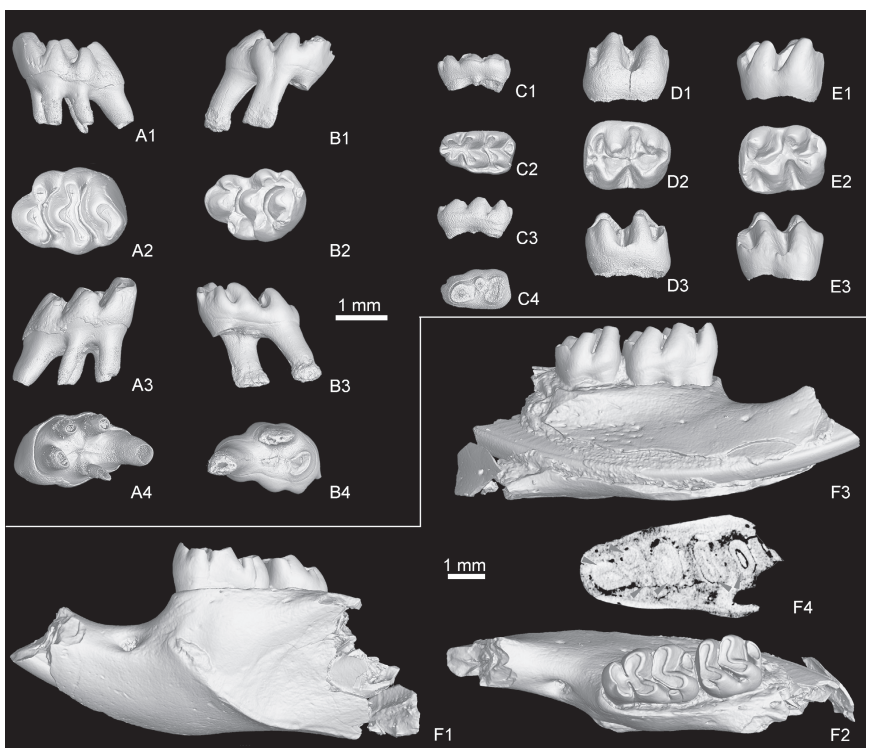


Fig. 6 Muridae remains from Yeka, Shangri-La, Yunnan
A, F. *Rattus pristinus*: A. right M1, IVPP V34067.1, F. left fragmentary mandible with i and m1–2, V34067.2;
B. *Apodemus latronum*, left M1, V34065; C. *Micromys minutus*, left m1, V34066;
D, E. *Cricetinus varians*: D. left M2, V34064.1, E. left m2, V34064.2
A1–F1. lingual views; A2–F2. occlusal views; A3–F3. buccal views; A4–C4. root views
F4 is CT slice of roots, red arrows show four roots of m1 and two roots of m2

wall of t2–t3 is straight. Cusp t1 is not connected to t5, but its posterobuccal corner is slightly connected to the anterolilngual wall of t5. Cusp t1 is far away from t4. Cusp t3 is far from the t6. A small spur is present posterior to t3. The posterior six main cusps form an incomplete stephanodont structure that separates t4 from the t7. Cusp t7 is ridge-like and elongated anteriorly. Cusp t12 is distinct. The posterior wall of the tooth is straight. The tooth has three roots, including an anterior, a posterior, and a lingual root.

Remarks This M1 represents the occurrence of a moderate-sized murid in the Yeka fossil assemblage. Its tooth pattern is incompletely stephanodont (t4 is not connected to t7). Cusp t1 is posterior to t2–t3, t7 is clearly anteroposteriorly elongated, t4 and t7 don't connect, t12 is developed, and the tooth has three roots. All these characters are identical to that of the extant *Apodemus latronum* (Wu, 2020). The known fossil material of this species was discovered from the fossil localities Wushan, Wanxian in Chongqing; Tongzi, Weining, Puding in Guizhou and Chenggong in Yunnan, with an age ranging from the Early to the Late Pleistocene (Zheng, 1993; Wu, 2020).

Genus *Rattus* Fischer, 1803

Rattus pristinus Jin et al., 2009

(Fig. 6A, F)

Referred specimen A right M1 from NXYK04, IVPP V34067.1; a left fragmentary mandible with i and m1–2 from NXYK03, V34067.2.

Measurements (in mm) M1: 3.0×1.85; dentary height beneath m1: 4.4; m1: 2.25×1.75; m2: 1.9×1.8.

Description On the M1, the main cusps are slightly oblique posteriorly and form three separate rows. The first row is formed by t1, t2, and t3. Cusp t1 is slightly convex and at the same level as t3, and both are slightly posterior to t2. Cusp t3 is closely attached to t2, and their anterior border is distinct and concave. There is no anterior cingulum, t1bis, t2bis, or posterior spurs of t1 or t3. The second row is formed by cusps t4, t5, and t6. Cusp t5 is the strongest and most anterior. Cusp t6 is slightly posterior to t4. The third row is formed by cusps t8 and t9. Cusp t7 is absent, while cusp t9 is significantly smaller than t8. The tooth has five roots, including a robust anterior, a linguocentral, a buccocentral, a linguoposterior, and a buccoposterior root.

The diastema length is greater than 3.0 mm. The mental foramen is located in the buccocentral part of the diastema, anterior to the m1. In the buccal view, the masseteric ridge has only one lower branch, and its apex is on the same vertical line as the anterior wall of the m1 and slightly higher than the mental foramen. The worn facet of the lower incisor is shaved. The m1 has a narrow anterior portion without an anterocentral cusp (Acc). The anterolingual cusp (Alc) is anterior to the anterobuccal cusp (Abc). The anterior mure (Am) between the paired anteroconid and protoconid-metaconid complex is clearly lingual. The longitudinal spur

(Ls) is absent. The posterior cingulid (Pcd) is large and centrally located. The buccal stylids have only c1, located on the anterobuccal side of the hypoconid. The m2 has a rectangular contour. The anterobuccal cusp is distinct. The Pcd is broad. Stylid c1 is present. m1 has four separate roots, including a strong anterior, a broad posterior, a long lingual, and a small buccal. The m2 has two roots, one anterior and one posterior.

Remarks The specimens illustrate the presence of a large-sized murid in the Yeka fossil assemblage. Given their simple dental morphology, particularly the presence of three transverse cusp rows on the M1 and the absence of an anterocentral cusp and anterior stylids on the m1, these teeth can be attributed to the genus *Rattus*. The tooth measurements of the Yeka material are notably smaller than those of *R. norvegicus* from Locality 1 of Zhoukoudian, Beijing, and Lower Cave of Yanjinggou, Chongqing. They are also slightly smaller than those of *R. rattus* from Upper Cave of Zhoukoudian. These measurements fall within the range observed for *R. pristinus* from the Early Pleistocene Fanchang locality in Anhui and *R. baoshanensis* from the Early Pliocene Baoshan locality in Yunnan (Zheng, 1993; Jin et al., 2009a; Chang et al., 2023). The Yeka material differs from *R. baoshanensis* in that it has four roots on M1, an absence of t7 and t12 on the M1, and an anterocentral cusp on the m1. Additionally, there is a strong connection among the paired anteroconid and protoconid-metaconid. The CT slice (Fig. 5F) of the mandible from Yeka demonstrate that its m2 has only two roots, which aligns with the diagnosis of *R. pristinus* but differs from the three roots observed in more derived species.

Order Carnivora Gray, 1821

Family Viverridae Gray, 1821

Genus *Paradoxurus* Cuvier, 1821

aff. *Paradoxurus* sp.

(Fig. 7J)

Referred specimen A half right M1 (lingual damaged) from NXYK02, IVPP V34070.

Measurements (in mm) Buccal mesiodistal length: 9.3, preserved buccal-lingual width: 9.7. A comparison of the measurements is presented in the following Table 3.

Description The tooth is bunodont, exhibiting two buccal main cusps of relatively rounded morphology and low ridges. The paracone is observed to be slightly larger than the metacone. The two main cusps are of a squat morphology and are separated from one another. The preparacrista and the postparacrista on the paracone are discernible, whereas the premetacrista and the postmetacrista on the metacone are inconspicuous. The parastyle is of a diminutive size and situated in front of the preparacrista, while the metastyle is located just behind the postmetacrista. The concave area at the center of the buccal margin is not readily apparent and therefore inconspicuous. The metaconule is larger than the paraconule. The central valley is enclosed by two transverse ridges, which are formed by the mesial postparaconule crista and the distal premetaconule crista. Additionally, a small valley is

present, which is limited by the preparaconule crista, the postparaconule crista, and the preparacrista. However, due to damage to the lingual portion, the development of the hypocone remains unknown.

Remarks Although the material is scarce, this partial tooth provides evidence of a viverrid from the Yeka locality. The preserved portion exhibits a deep central valley, a round paracone and metacone, and a cingulum at the buccal and anterobuccal sides of the paracone. It is evident that this specimen should be classified within the Viverridae rather than within other families of the Carnivora. The morphology of the tooth is comparable to those of *Paguma* or *Paradoxurus*.

The M1 of *Paguma* often exhibits a round triangular occlusal contour and lacks the cingulum at the buccal margin of the paracone. In contrast, the Yeka specimen displays a rather wide lingual portion and a developed buccal cingulum of the paracone, which differentiates it from *Paguma* but places it closer to *Paradoxurus*. In terms of size, the Yeka M1 is notably larger than those of *Paradoxurus* cf. *Par. hermaphroditus* from the Luobidong Cave, extant *Par. hermaphroditus*, *Paguma larvata* from the Xianrendong Cave, and *Pag. larvata* from Danyang (=Tanyang) (Table 3). Given the unavailability of sufficient material, the Yeka broken M1 is currently classified as an indeterminate species of *Paradoxurus* pending further investigation.

In the Quaternary geographical distribution, *Paguma* is considerably more widespread than *Paradoxurus*. The fossil record of *Paguma* and *Paradoxurus* is relatively sparse in China. The fossil *Paguma* has been discovered in a number of locations across China, including the Early Pleistocene Liucheng *Gigantopithecus* Cave in Guangxi, the late Early Pleistocene Fulongguan paleolithic site in Hubei, the late Middle Pleistocene Yixiantian Cave, the Late Pleistocene Danyang in Jiangsu, the Yangjiawan Cave 2 in Jiangxi, the Upper Cave and the Tianyuan Cave in Beijing, the Luobidong Cave in Hainan, the Holocene Xianrendong (=Hsienjen) Cave in Jiangxi, and the Gouwan Site in Henan (Huang and Ji, 1963; Pei, 1940, 1987; Tong et al., 2006; Wu et al., 2008; Jiangzuo et al., 2018; Hou et al., 2022; Pan et al., 2023). The *Paradoxurus* fossil has only been discovered in southern China, including the Middle to the early Late Pleistocene Wuyun Cave in Guangxi, the Late Pleistocene Luobidong Cave in Hainan, and the Mocun Cave in Guangxi (Hao and Huang, 1998; Chen et al., 2002; Fan et al., 2022). A comparison of the fossil and extant records indicated that *Paradoxurus* has

Table 3 M1 measurements of *Paradoxurus* and *Paguma* (mm)

Species	Locality	References	M1	
			Length	Width
aff. *Paradoxurus* sp.	Yeka	this text	9.3	>9.7
Paradoxurus cf. *Par. hermaphroditus*	Luobidong	Hao and Huang, 1998	6.3	7.9
Paradoxurus hermaphroditus	Extant	Shou, 1964	6.8	8.1
Paradoxurus hermaphroditus	OV1091(Extant)	this text	6.0	8.6
Paguma larvata	Danyang	Pei, 1940	6.4	8.6
Paguma larvata	Xianrendong	Huang and Ji, 1963	7.0	~7.9

a more limited geographic distribution than *Paguma*. *Paradoxurus* is more adapted to a warm forest environment in southern China and Southeast Asia.

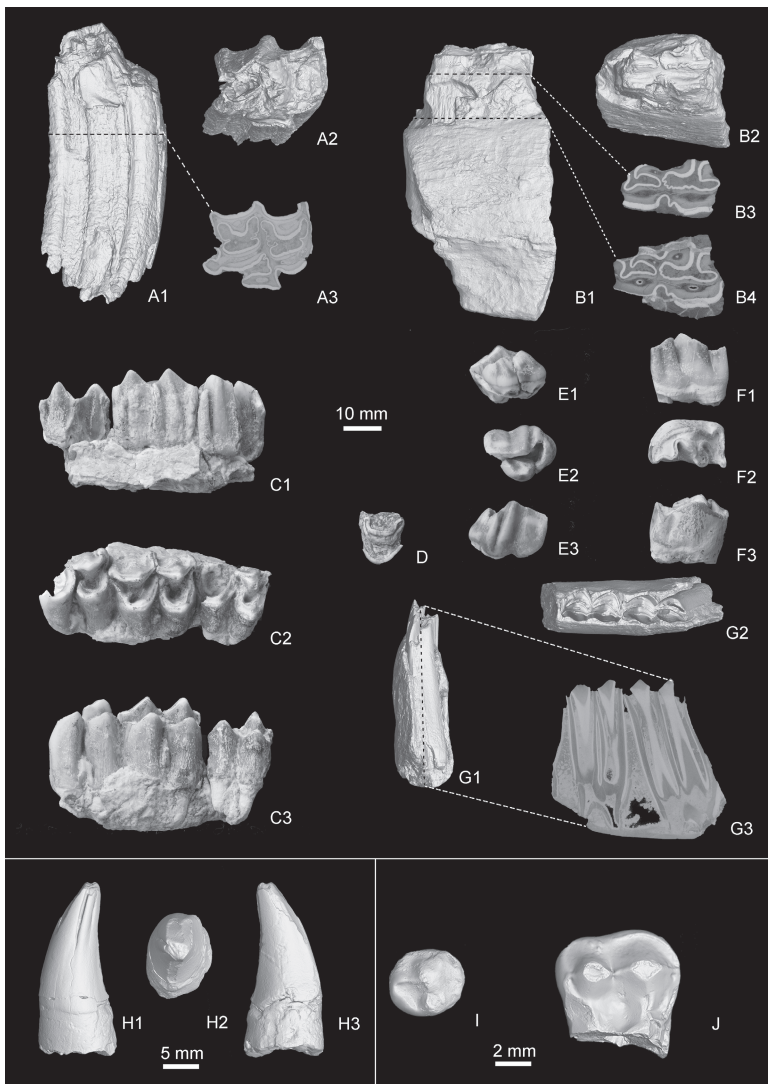


Fig. 7 Large mammal remains from Yeka, Shangri-La, Yunnan
A–B. *Equus yunnanensis*: A. left M3, IVPP V34072.1, B. left mandible with p2, V34072.2;
C–E. *Axis* cf. *A. shansius*: C. right maxilla with M1–3, V34073.1, D. left P2, V34073.2, E. right P3, V34073.3;
F. *Leptobos* sp., right p3, V34245; G. *Ovis* sp., right mandible with m2–3, V34074;
H, I. *Canis* sp.: H. left canine, V34071.1, I. left m3, V34071.2; J. aff. *Paradoxurus* sp., half right M1, V34070
A1–F1, H1 in lingual views, A2–H2, D, I, J in occlusal views, C3–F3, H3 in buccal views,
G1 in distal view. A3, B3, B4, G3 are CT slices

Family Canidae Gray, 1821

Genus *Canis* Linnaeus, 1758

Canis sp.

(Fig. 7H, I)

Referred specimen A left canine, IVPP V34071.1 and a left m3, V34071.2 from NXYK03.

Measurements (in mm) Canine, buccal crown height: 18.65, base length: 9.85, base width: 7.5; m3, occlusal length×width: 5.8×5.5.

Description The canine is moderately buccolingually compressed and exhibits a posterior curvature. An anterolingual ridge and two buccal grooves are present. The anterior wear facet is confined to the upper portion of the anterior wall of the tooth, whereas the posterior facet extends along with the posterior ridge of the tooth from the tip to the base.

The m3 exhibits a round occlusal contour, comprising two main cusps. The lingual cusp is larger and higher, representing the metaconid, while the buccal cusp is smaller and lower, corresponding to the protoconid. The trigonid basin is discernible. The posterior walls of the protoconid and the metaconid form an oblique slope. The tooth has a single root.

Remarks The dental morphology indicates that the two teeth are consistent with a species of the genus *Canis*. The species *Canis yuanmouensis* was designated by You and Qi (1973) and lacked the lower dentition in the original specimens. The Yeka material is not comparable to this species. The m3 of the *C. chihliensis* from the Early Pleistocene of Shanshenmiaozui in the Nihewan Basin exhibits a prominent protoconid at the center of the tooth, which differs from the buccally placed protoconid of the m3 from Yeka locality (Tong et al., 2012). The Yeka materials are most closely aligned with those of the species *C. teilhardi* from the Early Pleistocene of the Longdan locality in the Linxia Basin (Qiu et al., 2004), and the species *C. palmidens* from the Nihewan Basin (Teilhard de Chardin and Piveteau, 1930). Given the lack of available materials, the Yeka specimen is currently classified as an indeterminate species of *Canis*.

Order Artiodactyla Owen, 1848

Family Cervidae Gray, 1821

Genus *Axis* Smith, 1827

***Axis* cf. *A. shansius* Teilhard de Chardin & Trassaert, 1937**

(Fig. 7C–E)

Referred specimens Three specimens from NXYK03, including a fragmentary right maxilla with M1–3 (M1 and M3 broken, IVPP V34073.1), a broken left P2 (V34073.2), a right P3 (V34073.3).

Measurements (in mm) The length of M1–3: ~60; base length×width, M1: ~20.3×19.2, M2: 23.5×21.4, M3: ~20.7×20.7, P2: 12.2×14.1, P3: 16.3×16.8, lingual crown height, M1: 16.2, M2: 19.9, M3: 21.5.

Description The P2 is markedly worn with a length exceeding its width. The preserved lingual crown height is ~5.3 mm, exhibiting a U-shaped fossa and a small posterolingual crista.

The P3 exhibits a buccally projecting posterobuccal corner, which results in a notable

increase in the posterior width relative to the anterior width. The protocone is separated from the metaconule. The postprotocrista is absent. The premetaconulecrista is directed towards the metacone but is not attached to it. The anterior fossa and the posterior fossa are not completely separated by the premetaconulecrista. On the buccal side, the paracone, the metacone, and the metastyle form a high blade.

The three molars exhibit a comparable dental structure, with the exception of the M1, which lacks an entostyle. The molars display a trapezoidal occlusal contour, with a buccal width exceeding that of the lingual width. The parastyle, the mesostyle, and the metastyle are discernible. The buccal end of the postprotocrista is attached to the posterolingual wall of the paracone. The metaconule is observable on the M2.

Remarks The Yeka cervid specimens are identical to those of *Axis shansius* from the Xinyaozi Ravine of Tianzhen, Shanxi in both tooth dimension and morphology (Dong et al., 2020). This species was discovered from the Early Pleistocene of northern, central, and southwestern China (Teilhard de Chardin and Trassaert, 1937; Chia and Wang, 1978; Dong and Fang, 2004; Dong, 2006; Bai et al., 2017). In Yunnan Province, *A. shansius* has been discovered in the Yuanmou Man Site (Lin et al., 1978).

Family Bovidae Gray, 1821

Genus *Leptobos* Rütimeyer, 1878

Leptobos sp.

(Fig. 7F)

Referred specimens A right p3 from NXYK03, IVPP V34245.

Measurements (in mm) Base length×width, p3: 19.9×11.3; lingual crown height, p3: 14.2.

Description The p3 exhibits a round anterobuccal margin and an almost straight posterior margin. The anterior portion is constituted by the anterior stylid, the anterior conid, and the anteriobuccal cristid. The middle portion is constituted by a large mesobuccal conid, a round mesolingual conid, and a short and oblique transverse cristid. Neither an anterolingual nor a posterolingual cristid is present. The posterobuccal cristid is oblique in orientation. The posterior portion of the p3 is formed by the fused posterolingual conid, the posterobuccal conid, and the posterior stylid. The anterobuccal, anterolingual, and posterobuccal cingulids are absent. The anterior valley is wide, while the posterior valley is narrow and curved anterobuccally. The back valley is absent. The crown walls are covered a thin layer cements. This specimen has two roots.

Remarks This specimen is identical to those of *Leptobos* sp. from the Jianshi Hominid site in Hubei, both in dimensions and morphology (Chen, 2004). Fossils of *Leptobos* have been found in the Early Pleistocene deposits of northern, central, and southwestern China (Chi, 1975; Hu and Qi, 1978; Chia and Wang, 1978; Qiu et al., 2004; Dong, 2008; Dong et al., 2009;

Li, 2015). Within Yunnan Province, *Leptobos* sp. was discovered at the Zhongdian locality (Ma et al., 2004).

Family Bovidae Gray, 1821

Genus *Ovis* Linnaeus, 1758

Ovis sp.

(Fig. 7G)

Referred specimen A right fragmentary mandible with m2–3, m3 posteriorly broken, collected in 2024 (equal to the layer of NXYK03), IVPP V34074.

Measurements (in mm) Dentary height beneath m2: 33.9; dentary buccolingual thickness: 14.6; m2 crown height: 39.0, length×width: 16.4×8.05; m3 crown height: 41.7, preserved length: 17.0, width: 7.0.

Description The dentary only preserves a posterior portion of the horizontal ramus and the posterior two molars. The molars are extremely high crowned. On the m2, the four main cusps enclose two fossae, the anterior and the posterior. The anterior cingulid, the mesostylid, the metastylid, and the entostylid are present. The external postprotocristid, external postmetacristid, ectostylid, and posterior ectostylid are absent. The postentocristid is not fused with the posthypocirstid. The anterior portion of the m3 has a similar morphology to that of the m2, but it is distinctly elongated.

Remarks The specimen is distinguished by the high crowns of its molars and a relatively simple occlusal pattern. It can be readily assigned to the tribe Caprini and most closely resembles those of *Ovis*. A number of species of *Ovis* have been documented from the Early Pleistocene deposits at Wangbuding, Dege, Sichuan (Zong et al., 1996). However, the tooth measurements of the Yeka specimen's tooth are smaller than those of the Wangbuding locality. Given the lack of available materials, the Yeka specimen is currently classified as an indeterminate species of *Ovis*.

Order Perissodactyla Owen, 1848

Family Equidae Gray, 1821

Genus *Equus* Linnaeus, 1758

Equus yunnanensis Colbert, 1940

(Fig. 7A, B)

Referred specimen An isolated left M3, collected in 2024, from the upper part of the section in Zong et al. (1996), IVPP V34072.1; a fragmentary left mandible with p2 from NXYK03, V34072.2.

Measurements (in mm) M3 occlusal length×width: 31.2×24.8, PL (protocone length): 10.6, PI (protocone index, protocone length/tooth length): 34%; p2: 34×16.4, FL (postflexid length): 16.4, FI (postflexid index, postflexid length/tooth length): 48%.

Description On the M3, the posterior portion of protocone is elongated, exhibiting

a straight lingual contour and a pointed termination. The postflex is deep and wide at the base. The pli caballine is single and diminutive. The hypocone is rounded and blunt, with no discernible constriction. The parastyle is elongated and extends labially. The mesostyle is of a short and wide configuration. The buccal wall is curved, wide, and shallow.

On the p2, the paraconid is notable for its large size, subtriangular shape, lingual extension, and buccal connection with the protoconid. The metaconid is of a diminutive, oval shape. The metastylid is of considerable size and possesses a leaf-like shape with a relatively short stem. It extends to a greater extent lingually than the metaconid. The linguaflexid opens in a wide V-shaped direction towards the anterobuccal side. The entoconid is notably large and irregular in shape. The hypoconulid is pointed in shape. The protoconid is narrow and exhibits slight swelling of the lingual and labial walls. The hypoconid is elongated with thick lingual and buccal enamel. The pli caballinid is strong. The ectoflexid is shallow and situated distant from the isthmus. The horns of the preflexid are asymmetric, with the posterior horn being elongated and extending anterobuccally, while the anterior horn is shorter. The postflexid is elongated and displays a swollen base.

Remarks In consideration of the tooth dimensions and morphology, the two specimens can be attributed to the species *Equus yunnanensis*. This species is distinguished by the following characteristics: The cheek teeth are medium-sized, with a medium-length protocone. Enamel plications are typically strong, and the linguaflexid is V-shaped. The metaconid and metastylid are highly rounded, while the ectoflexid is shallow-rarely penetrating the isthmus, even on lower molars. The pli caballinid is weak. (Deng and Xue, 1999). Four postcranial bones, a maxilla, and six isolated teeth of *E. yunnanensis* have been identified from the Yeka locality in 1985 (Zong et al., 1996).

Rhinocerotidae Owen, 1845

Rhinocerotidae gen. et sp. indet.

Remarks The remains of a few tooth enamel fragments represent the appearance of a rhinoceros in the Yeka locality.

5 Discussion

5.1 Faunal composition

Zong (1987a) described nine species of the fossil collection from the Yeka locality, including *Mimomys hengduanshanensis*, *Hyaena licenti*, *Metailurus*? sp., *Canis* sp., *Equus yunnanensis*, *Cervus* cf. *C. elegans*, *Gazella* sp., *Bos* (*Bibos*) sp., and Bovinae indet. Zheng (2020) reidentified *Mimomys hengduanshanensis* as *Villanyia hengduanshanensis*. Qiu (2000) reidentified *Cervus* (*Rusa*) *elegans* as *Pseudodama elegans*. Qiu et al. (2004) reidentified *Hyaena licenti* as *Pachycrocuta pyrenaica*. The novel findings from the Yeka locality collected

in 2020 and 2024 have been identified as belonging to 5 orders, 12 families, 15 genera, and 15 species. The following have been already reported in Zong's pioneering works (Zong, 1987a; Zong et al., 1996): *Villanyia hengduanshanensis*, *Pachycrocuta pyrenaica*, *Equus yunnanensis*, *Pseudodama elegans*, *Gazella* sp., *Bos* (*Bibos*) sp., *Metailurus*? sp., *Canis* sp. and Rhinocerotidae gen. et sp. indet. The remaining species represent the first discovery of these fossils in the Yeka locality or the Pleistocene of the Hengduan Mountains. The Yeka Fauna lacks evidence of typical Pliocene elements. The co-occurrence of *Ochotonoides complicidens*, *Mimomys* (*Cromeromys*) *gansunicus*, *Cricetinus varians*, *Rattus pristinus*, *Equus yunnanensis*, and *Axis shansius* confirms that the biochronology of the Yeka Fauna should be strictly limited to the Early Pleistocene.

5.2 Faunal correlation

The Zhongdian Fauna was designated by Ma et al. (2004). They reported the discovery of the Zhongdian Fauna at a brick field situated approximately 6 km south of the urban center of Shangri-La. The Zhongdian Fauna comprises 11 genera and 11 species of mammals. Nine species have been subjected to detailed descriptive analysis. The following species are identified: *Procynocephalus* cf. *P. wimani*, *Hystrix* sp., *Equus yunnanensis*, *Cervavitus ultimus*, *Eucladoceros* sp., *Cervus* (*Rusa*) *yunnanensis*, *Muntiacus* sp., *Gazella* sp., and *Leptobos* sp. The material awaiting description includes coprolites from *Hyaena*, incisor and limb bones of carnivores, cheek teeth fragments of rhinoceros, and some limb bones of artiodactyls. The biochronology of the Zhongdian Fauna is estimated to be the Early Pleistocene. Due to the sampling bias or specific entombment, the Zhongdian Fanua is predominantly comprised of large mammals, particularly cervids and bovids. The Yeka Fauna (see the updated fossil list in the Table 4) shares *Equus yunnanensis* at the species level and *Canis*, *Cervus*, *Gazella* and *Leptobos* at the genus level with the Zhongdian Fauna. However, due to the predominant species being different in the Yeka and Zhongdian faunas, further comparison is limited.

The Wangbuding Fauna is another Early Pleistocene fauna discovered during the Hengduan Mountains Scientific Expedition, which was led by Zong's group in the 1980s (Zong et al., 1996). The Wangbuding locality is situated at the Wangbuding village, Dege County, Sichuan Province, and approximately 450 km northwest of the Nixi locality. The fauna comprises 17 genera and 19 species, including *Ochotona hengduanshanensis*, *Mimomys* cf. *M. hengduanshanensis*, *Hypolagus* cf. *H. schreuderi*, *Indarctos*? sp., *Ursus* cf. *U. thibetanus*, *Martes* cf. *M. pachygnatha*, *Meles chiai*, *Hyaena licenti*, *Metailurus hengduanshanensis*, *Homotherium hengduanshanensis*, *Lynx shansius*, *Panthera pardus*, *Sivapanthera pleistocaenicus*, *Postschizotherium tibetensis*, *Munitacus lacustris*, *M. hengduanshanensis*, *Gazella* sp., *Ovis* cf. *O. shantongensis*, *Ovis*? sp., and *Spirocerus*? sp. Chen (2003) reidentified *Postschizotherium tibetensis* as *Hengduanshanhyrax tibetensis*. Zheng (2020) proposed a transfer of *Mimomys* cf. *M. hengduanshanensis* to *Villanyia hengduanshanensis*. Qiu et al.

(2004) reidentified *Hyaena licenti* as *Pachycrocuta pyrenaica*. Due to the sampling bias or specific entombment, the Wangbuding Fanua is predominantly comprised of abundant carnivores. The Yeka Fauna shares *Villanyia hengduanshanensis*, *Pachycrocuta pyrenaica* and *Hypolagus* cf. *H. schreuderi* at the species level and *Gazella*, and *Ovis* at the genus level with the Wangbuding Fauna.

Table 4 Composition of the Yeka Fauna and comparison with other Early Pleistocene faunas

Yeka (this paper)	Yeka (Zong, 1987a)	Zhongdian (Ma et al., 2004)
Rodentia	Rodentia	Rodentia
Arvicolidae	Arvicolidae	Hystricidae
Villanyia hengduanshanensis	*Villanyia hengduanshanensis*	*Hystrix* sp.
Mimomys (*Cromeromys*) *gansunicus*	Carnivora	Primates
Rhizomyidae	Canidae	Cercopithecidae
Rhizomys pruinosus	*Canis* sp.	*Procynocephalus* cf. *P. wimani*
Cricetidae	Felidae	Perissodactyla
Cricetinus varians	*Metailurus*? sp.	Equidae
Muridae	Hyaenidae	*Equus yunnanensis*
Apodemus latronum	*Hyaena licenti*	Rhinocerotidae indet.
Micromys minutus	Perissodactyla	Artiodactyla
Rattus pristinus	Equidae	Cervidae
Lagomorpha	*Equus yunnanensis*	*Cervus* (*Rusa*) *yunnanensis*
Ochotonidae	Artiodactyla	*Cervavitus ultimus*
Ochotonoides complicidens	Cervidae	*Eucladoceros* sp.
Leporidae	*Pseudodama elegans*	*Muntiacus* sp.
Hypolagus cf. *H. schreuderi*	Bovidae	Bovidae
Carnivora	Bovinae indet.	*Gazella* sp.
Viverridae	*Gazella* sp.	*Leptobos* sp.
aff. *Paradoxurus* sp.	*Bos* (*Bibos*) sp.	
Canidae		
Canis sp.		
Perissodactyla		
Equidae		
Equus yunnanensis		
Artiodactyla		
Cervidae		
Axis cf. *A. shansius*		
Bovidae		
Ovis sp.		
Leptobos sp.		

The Longdan Fauna is an Early Pleistocene mammalian fauna from the Wucheng Loess in the Linxia Basin, Gansu Province. It comprises 33 species belonging to 6 orders, 16 families, and 29 genera (Qiu et al., 2004, 2009; Wang, 2005). As a consequence of sampling bias (collecting "dragon bones" for traditional Chinese medicine), the Longdan Fauna is dominantly comprised of abundant carnivores, perissodactyls, and artiodactyls. The Yeka Fauna shares *Mimomys* (*Cromeromys*) *gansunicus* at the species level and *Equus*, *Pachycrocuta*, *Pseudodama Canis*, and *Gazella Leptobos* at the genus level with the Longdan Fauna.

The Nihewan Fauna (sensu stricto) is a classical Early Pleistocene fauna from northern China, comprising at least 42 species (Qiu, 2000; Cai et al., 2013). The Yeka Fauna shares *Ochotonoides complicedens* and *Pseudodama elegans* at the species level and *Canis*, *Pachycrocuta*, *Equus*, *Cervus* (*Rusa*), *Gazella*, and *Ovis* at the genus level with the Nihewan Fauna.

The Renzidong Cave Fauna is a very important Early Pleistocene Fauna in southern China. After four years of investigation and excavation, more than 7000 specimens were obtained from the Renzidong Cave. Among them, mammalian fossil specimens include 9 orders, 28 families, 70 genera, and 74 species (Jin and Liu, 2009). Typical boreal and austral elements, as well as widespread elements coexist in this fauna. This reflects the transitional characteristics of the fauna between the Palaearctic and Oriental regions. The Yeka Fauna shares *Mimomys* (*Cromeromys*) *gansunicus*, *Cricetinus varians*, and *Rattus pristinus* at the species level, and *Villanyia*, *Hystrix*, *Apodemus*, *Micromys*, *Hypolagus*, *Rhizomys*, *Equus*, *Cervus*, and *Bos* (*Bibos*) *Leptobos* at the genus level with the Renzidong Cave Fauna.

The Tuozidong Fauna is one of the few Early Pleistocene mammalian faunas in the lower valleys of the Yangzi River. It includes 6 orders, 14 families, 24 genera, and 26 species (Nanjing Museum and Institute of Archaeology, Jiangsu Province, 2007). The Yeka Fauna shares *Axis shansius* at the species level, and *Equus*, *Bos* (*Bibos*), *Leptobos Pachycrocuta*, and *Gazella* at the genus level with the Tuozidong Fauna.

The Yuanmou Man Fauna is notable for the discovery of the earliest *Homo* fossils (two teeth) in China. The Yuanmou Man Site is located in the Yuanmou Basin, central of Yunnan Province, and is approximately 335 km southeast of the Nixi locality. You and Qi (1973) first reported the associated mammal fossils of *Homo*, which comprised 10 families, 12 genera, and 16 species. Lin et al. (1984) provided an updated fossil list, which includes 18 families, 24 genera, and 28 species. Qiu et al. (2004) reidentified *Hyaena licenti* as *Pachycrocuta pyrenaica*. The Yeka Fauna shares *Ochotonoides complicidens*, *Equus yunnanensis*, *Pachycrocuta pyrenaica* and *Axis shansius* at the species level and *Rhizomys*, *Canis*, *Cervus* (*Rusa*), *Bos* (*Bibos*), and *Gazella* at the genus level with the Yuanmou Man Fauna of Lin et al. (1978). Furthermore, although different species of viverrids were identified in the Yeka and the Yuanmou Man faunas, the presence of viverrids in both faunas suggests a certain degree of similarity in the paleoenvironments during the Early Pleistocene in central and northwestern Yunnan.

In brief, the Yeka Fauna is most closely correlated to the Yuanmou Man Fauna when compared to the Early Pleistocene Zhongdian, Wangbuding, Longdan, Nihewan (sensu stricto), Renzidong Cave, Tuozidong and Yuanmou Man faunas.

5.3 Paleobiogeography and paleoenvironment

Both boreal and austral elements are present in the Shangri-La fossil mammal assemblage. In the fossil assemblage of the Yeka locality, *Mimomys* (*Cromeromys*) *gansunicus*,

Cricetinus varians, *Ochotonoides complicidens*, *Hypolagus* cf. *H. schreuderi*, *Pachycrocuta pyrenaica*, *Axis shansius*, and *Pseudodama elegans* can be identified as boreal taxa, while *Rhizomys pruinosus*, *Hystrix* sp., *Apodemus latronum*, *Rattus pristinus*, aff. *Paradoxurus* sp., *Equus yunnanensis*, and *Cervus* (*Rusa*) *yunnanensis* are identified as austral taxa. *Micromys minutus* is a cosmopolitan species. *Procynocephalus* cf. *P. wimani* and *Cervavitus ultimus* may be adapted to both boreal and austral regions (see Table 5). Norton et al. (2010) proposed a spatial division of the Palearctic and the Oriental regions in Quaternary China, which they identified as a biogeographic boundary situated between the Yangtze River and the Qinling Mountain Range. This boundary seems to traverse the Hengduan Mountain Range, though it is not an absolute delineation. In contemporary biogeography, the central region of the Hengduan Mountains is typically regarded as a transitional zone between the Oriental and Palearctic realms in China (Chen et al., 2008). The Yeka Fauna demonstrates a distinctive combination of boreal and austral elements, suggesting the existence of a transitional zone in the Early Pleistocene era within the central Hengduan Mountains.

Prior research conducted by Zong's group posited that during the Early Pleistocene, the Nixi region was situated within a transitional zone between the northern subtropical and warm temperate climates, exhibiting a vertical zonation of vegetation (Zong, 1987a; Zong et al., 1996). The paleoelevation of the Yeka fossil locality in the Early Pleistocene was estimated to be no more than 1500 m, which is notably lower than the current altitude of 3750 m.

Our analysis suggests that the Yeka Fauna reflects a moderate-elevation montane forest mixed with a grassland landscape during the Early Pleistocene. The paleoaltitude of the Yeka fossil site during the Early Pleistocene is estimated to not have exceeded 3000 m. The reasons for this conclusion are as follows: the extant *Apodemus latronum* is primarily distributed to the montane forests and adjacent meadows in southwestern China and northern Myanmar, with an altitude range of 2700 to 4000 m (Smith and Xie, 2013; Denys et al., 2017); *Micromys minutus* is a widely distributed species that has adapted to low-altitude grassland and shrubland habitats, its upper altitude limit is approximately 1700 m (Denys et al., 2017); *Rhizomys pruinosus* is adapted to the low-elevation bamboo thickets or beardgrass of the Oriental region of China, India-China Peninsula, and northwestern India; in China, *R. pruinosus* is distributed to the upper altitude limit of 1000 m, while in northeastern India it is distributed to an altitude of 1500 m (Norris, 2017); living viverrids are typically found in warm forests at low-elevation; the upper altitude limit for the distribution of *Paguma larvata* and *Paradoxurus hermaphroditus* is both below 2500 m (Jennings and Veron, 2009); *Equus yunnanensis* is typically regarded as a grazer that has adapted to an open, grassy habitat; the isotope analysis of tooth enamel from *E. yunnanensis* specimens from the 1.7 Ma Yuanmou locality indicates notable seasonal fluctuations in dietary patterns (Biasatti et al., 2012); the presence of ochotonid (*Ochotonoides complicidens*), leporid (*Hypolagus* cf. *H. schreuderi*) and high-

crowned arvicolids (*Villanyia hengduanshanensis* and *Mimomys* (*Cromeromys*) *gansunicus*) indicates the existence of open grassland.

Table 5 Zoogeographical attributions of fossil mammalian species in Shangri-La region

Species	Boreal/Austral/ Endemic	Localities	References
†*Procynocephalus* cf. *P. wimani*	Cosmopolitan (Austral+Boreal)	Zhongdian, Yunnan	Ma et al., 2004
		Fanchang, Anhui	Jin et al., 2000
		Wushan, Sichuan	Jin et al., 2000
		Xin'an, Henan	Schlosser, 1924
		Loc. 12. Zhoukoudian, Beijing	Teilhard de Chardin, 1938
		Beigudi(=Peikuti), Hebei	Young and Pei, 1933
		Wushan, Chongqing	Huang et al., 1991
†*Villanyia hengduanshanensis*	Endemic	Nixi, Yunnan	Zong, 1987a; This paper
		Dege, Sichuan	Zong et al., 1996
†*Mimomys* (*Cromeromys*) *gansunicus*	Boreal	Nixi, Yunnan	This paper
		Lingtai, Gansu	Zheng and Zhang, 2000
		Heshui, Gansu	Zheng, 1976
		Longdan, Gansu	Qiu et al., 2004
		Mianxian, Shaanxi	Tang et al., 1988
		Nihewan Basin, Hebei	Cai et al., 2007, 2008
		Yushe Basin, Shanxi	Zhang, 2017
		Fanchang, Anhui	Jin et al., 2009a
†*Rhizomys pruinosus*	Austral	Nixi, Yunnan	This paper
		Chenggong, Yunnan	Qiu et al., 1984
†*Cricetinus varians*	Boreal	Nixi, Yunnan	This paper
		Zhoukoudian, Beijing	Zheng, 1984
		Lantian, Shaanxi	Chi, 1974; 1975; Hu and Qi, 1978
		Nihewan Basin, Hebei	Gai and Wei, 1977
		Anping, Liaoning	Zhang et al., 1980
		Xiaogushan, Liaoning	Zhang et al., 1985
		Hexian, Anhui	Zheng, 1983
		Wuhu, Anhui	Jin et al., 2004
		Fanchang, Anhui	Jin et al., 2009a
Apodemus latronum	Austral (fossil)	Nixi, Yunnan	This paper
		Longgupo, Chongqing	Zheng, 1993
		Baotansi, Chongqing	Zheng, 1993
		Yanjinggou, Chongqing	Zheng, 1993
		Tianmen Cave, Guizhou	Zheng, 1993
		Tianqiao, Guizhou	Zheng, 1993
		Chuan Cave, Guizhou	Zheng, 1993
		Chenggong, Yunnan	Qiu et al., 1984
	Austral (extant)	Gansu, Shanxi, Chongqing, Guizhou, Sichuan, Xizang, Yunnan, Hubei	Wei et al., 2022
Micromys minutus	Austral (fossil)	Nixi, Yunnan	This paper
		Chenggong, Yunnan	Qiu et al., 1984
		Yushe Basin, Shanxi	Wu et al., 2017
		Puding, Guizhou	Zheng, 1993
		Jianshi, Hubei	Zheng, 2004
		Panxian, Guizhou	Zhang et al., 1997
		Fusui, Guangxi	Wang et al., 2021
	Cosmopolitan (extant)	Hei longjiang, Jilin, Liaoning, Hebei, Nei Mongol, Taiwan	Wei et al., 2022
†*Rattus pristinus*	Austral	Nixi, Yunnan	This paper
		Fanchang, Anhui	Jin et al., 2009a

Continued

†*Ochotonoides complicidens*	Boreal	Nixi, Yunnan	This paper
		Qingyang, Gansu	Boule and Teilhard de Chardin, 1928
		Nihewan Basin, Hebei	Teilhard de Chardin and Piveteau, 1930
		Yulin, Shaanxi	Teilhard de Chardin and Young, 1931
		Jingle, Shanxi	Teilhard de Chardin and Young, 1931
		Loc. 18. Zhoukoudian, Beijing	Teilhard de Chardin, 1940
		Yushe Basin, Shanxi	Teilhard de Chardin, 1942; Wu and Flynn, 2017a
		Dalian, Liaoning	Jin et al., 2021
		Lantian, Shaanxi	Chow and Li, 1965; Ji, 1976; Hu and Qi, 1978
		Heshui, Gansu	Zheng, 1976
		Luochuan, Shaanxi	Zheng et al., 1985b
		Guide, Qinghai	Zheng et al., 1985a
		Dali, Shaanxi	Wang, 1988
		Yunxian, Hubei	Liu and Zheng, 1997
		Lingtai, Gansu	Zheng and Zhang, 2000, 2001; Erbajeva and Zheng, 2005
†*Hypolagus* cf. *H. schreuderi*	Boreal	Nixi, Yunnan	This paper
		Dege, Sichuan	Zong et al., 1996
		Zhoukoudian, Beijing	Teilhard de Chardin, 1940
aff. *Paradoxurus* sp.	Austral	Nixi, Yunnan	This paper
		Bubing Basin, Guangxi	Wang et al., 2007
		Tiandong, Guangxi	Chen et al., 2002
		Lufeng, Yunnan	Qi, 1985
Metailurus? sp.	Boreal	Nixi, Yunnan	Zong, 1987a
		Baode, Shanxi	Zdansky, 1924
		Qingyang, Gansu	Zdansky, 1924
		Xinan, Henan	Zdansky, 1924
		Dege, Sichuan	Zong et al., 1996
		Yushe Basin, Shanxi	Chang and Liu, 1964
		Jingle, Shanxi	Chen, 1994
		Yuanmou, Yunnan	Zong and Jiang, 1991
†*Pachycrocuta pyrenaica*	Boreal	Nixi, Yunnan	Zong, 1987a
		Dege, Sichuan	Zong et al., 1996
		Wushan, Chongqing	Huang and Fang, 1991
		Nihewan Basin, Hebei	Liu et al., 2022
		Yushe Basin, Shanxi	Qiu, 1987
†*Equus yunnanensis*	Austral	Nixi, Yunnan	Zong, 1987a; This paper
		Zhongdian, Yunnan	Ma et al., 2004
		Yuanmou, Yunnan	Liu and You, 1974
		Liucheng, Guangxi	Pei, 1961
		Jianshi, Hubei	Xu et al., 1974
		Yunxian, Hubei	Li et al., 1994
		Yanyuan, Sichuan	Zong, 1987b
		Wushan, Chongqing	Huang and Fang, 1991
†*Axis shansius*	Boreal	Nixi, Yunnan	This paper
		Nihewan Basin	Teilhard de Chardin and Piveteau, 1930
		Yushe Basin	Teilhard de Chardin and Trassaert, 1937
		Xihoudu, Shanxi	Chia and Wang, 1978
		Lantian, Shaanxi	Chi, 1975
		Yuanmou, Yunnan	Lin et al., 1978
		Tangshan, Nanjing	Dong and Fang, 2004
		Xuchang, Henan	Dong and Li, 2009
		Dalian, Liaoning	Liu et al., 2017; Bai et al., 2017
		Tianzhen, Shanxi	Dong et al., 2020

Continued

†*Leptobos* sp.	Cosmopolitan	Nixi, Yunnan	This paper
		Lantian, Shaanxi	Hu and Qi, 1978; Chi, 1975
		Xihoudu, Shanxi	Chia and Wang, 1978
		Longdan, Gansu	Qiu et al., 2004; Li, 2015
		Fanchang, Anhui	Dong et al., 2009
		Jianshi, Hubei	Chen, 2004
†*Pseudodama elegans*	Boreal	Nixi, Yunnan	Zong, 1987a
		Nihewan Basin, Hebei	Teilhard and Piveteau, 1930
†*Cervus* (*Rusa*) *yunnanensis*	Austral	Nixi, Yunnan	Zong, 1987a
		Zhongdian, Yunnan	Ma et al., 2004
		Yuanmou, Yunnan	Lin et al., 1978
		Jianshi, Hubei	Chen, 2004
		Liucheng, Guangxi	Han, 1987
		Chongzuo, Guangxi	Jin et al., 2009b
†*Cervavitus ultimus*	Cosmopolitan	Zhongdian, Yunnan	Ma et al., 2004
		Tangshan, Nanjing	Dong and Fang, 2004
		Wushan, Chongqing	Huang and Fang, 1991
		Yuanmou, Yunnan	Liu and You, 1974

It is very noteworthy that primate fossils were found at the Early Pleistocene strata in Shangri-La. Currently, two fossil species of Papionini primates have been discovered in the Shangri-La area. A pair of mandibular fragments belonging to a *Papio*-like primate was unearthed from an unidentified site along the Jinsha River (Zheng et al., 2006). The specimen exhibits a high degree of dentary morphological similarity to that of the extant *Papio hamadryas ursinus*. Another fossil of a Papionini primate is that of *Procynocephalus* cf. *P. wimani* from the Zhongdian Fauna (Ma et al., 2004). *Procynocephalus* fossil has been predominantly discovered in the Late Pliocene to the Early Pleistocene of East and South Asia. They are regarded as a terrestrial primate that consumed hard food (Takai, 2008; Kostopoulos et al., 2018). *Procynocephalus wimani* has been identified in a number of locations in China, including Xin'an, Jingxing, Renzidong Cave, Zhoukoudian loc.12, Wushan, and Zhongdian (Schlosser, 1924; Young and Pei, 1933; Teilhard de Chardin, 1938; Jin et al., 2000; Ma et al., 2004), and Lang Trang, Vietnam (Pope et al., 2000). The discovery of two Papionini primates in the Shangri-La area suggests that the region was characterized by relatively open habitats rather than dense forests during the Early Pleistocene. Zheng et al. (2006) proposed that the Shangri-La area may have served as a significant migratory route for the settlement of East Asia by hominins and other primates. Further research should prioritize the excavation of additional primate fossils in the Shangri-La region or the Hengduan Mountains.

6 Conclusion

The recent findings from the 2020 and 2024 field seasons in the Yeka locality, Nixi, Shangri-La, northwestern Yunnan, have identified a total of 15 species. In combination with the previous fossil list (Zong, 1987a; Zong et al., 1996), the Yeka Fauna currently comprises 20 species. The new fossils provide further confirmation of the biochronology of the Yeka

Fauna, which is in the Early Pleistocene. In comparison to the Early Pleistocene faunas from Zhongdian, Wangbuding, Longdan, Nihewan (sensu stricto), and the Yuanmou Man Site, the Yeka Fauna is most closely correlated to the Yuanmou Man Fauna. The occurrence of boreal and austral elements in the Yeka Fauna is analogous to the contemporary biogeographic pattern observed in the Hengduan Mountains. The Yeka Fauna encompasses both forest and grassland-adapted elements, indicating a moderate-elevation montane forest mixed with a grassland landscape during the Early Pleistocene.

Acknowledgements We acknowledge with gratitude Dr. Hou Yemao and Mrs. Yin Pengfei for their valuable assistance in performing the CT scans, as well as Mr. Li Dongsheng and Mrs. Chen Jin for their help with specimen comparison. We also extend our sincere gratitude to the two reviewers for their constructive comments.

滇西北香格里拉叶卡地点早更新哺乳动物化石

张立民[1,4]　常美静[1,4]　鲁　丹[1,4]　巩　皓[1,4]　秦　超[1,4]　高　峰[2]　潘高原[3]
李　钢[3]　邓　涛[1,4]　史静耸[5]　倪喜军[1,4]　李　强[1,4]

(1 中国科学院古脊椎动物与古人类研究所，脊椎动物演化与人类起源重点实验室 北京 100044)

(2 云南省文物考古研究所 昆明 650118)

(3 云南省迪庆藏族自治州文物管理所 香格里拉 674400)

(4 中国科学院大学 北京 100049)

(5 中国科学院动物研究所 北京 100101)

摘要：早更新世叶卡动物群最早发现于20世纪80年代的横断山科学考察中。第二次青藏高原科学考察期间，2020和2024年两次采集到的新的哺乳动物化石标本，经鉴定包含了5目、12科、15属、15种。与中国典型的早更新世哺乳动物群的对比表明，香格里拉地区的化石哺乳动物组合在组成上最接近于元谋人动物群。香格里拉化石哺乳动物组合在动物地理上以南北混合为显著特征，这种模式与横断山现代动物地理格局高度相似。动物组成分析结果反映出早更新世时期，香格里拉地区呈现中等海拔森林和草原镶嵌的环境。

关键词：香格里拉，早更新世，叶卡动物群，横断山，古环境

中图法分类号：Q915.873　　**文献标识码**：A　　**文章编号**：2096–9899(2026)03–0254–40

References

Averianov A O, 1996. On the systematic position of rabbit "*Caprolagus*" *brachypus* Young, 1927 (Lagomorpha, Leporidae) from the Villafranchian of China. Russ Acad Sci Proc Zool Inst, St Petersburg, 270: 148–157

Bai W P, Dong W, Liu J Y et al., 2017. New material of *Axis shansius* (Mammalia, Artiodactyla) and phylogenetic consideration of *Axis*. Quat Sci, 37: 821–827

Bärmann E V, Rössner G E, 2011. Dental nomenclature in Ruminantia: towards a standard terminological framework. Mamm Biol, 76: 762–768

Biasatti D, Wang Y, Gao F et al., 2012. Paleoecologies and paleoclimates of late Cenozoic mammals from Southwest China: evidence from stable carbon and oxygen isotopes. J Asian Earth Sci, 44: 48–61

Boufford D E, Van Dyck P P, 2000. South-central China. In: Mittermeier R A, Myers N, Mittermeier C G eds. Hotspots: Earth's Biologically Richest and Most Endangered Terrestrial Ecoregions. Mexico City: CEMEX. 338–351

Boule M, Teilhard de Chardin P, 1928. Paléontologie. In: Boule M, Breuil H, Licent E et al. eds. Le Paléolithique de la Chine. Paris: Archives de l'Institut de Paléontologie Humaine. 27–102

Cai B Q, Zheng S H, Li Q, 2007. Plio-Pleistocene small mammals from the Niutoushan section of the Yuxian basin, China. Vert PalAsiat, 45: 232–245

Cai B Q, Li Q, Zheng S H, 2008. Fossil mammals from Majuangou section of Nihewan basin, China and their age. Acta Anthrop Sin, 27: 127–140

Cai B Q, Zheng S H, Liddicoat J C et al., 2013. Review of the litho-, bio-, and chronostratigraphy in the Nihewan Basin, Hebei, China. In: Wang X M, Fortelius M, Flynn L J eds. Fossil Mammals of Asia: Neogene Biostratigraphy and Chronology. New York: Columbia University Press. 218–242

Chang H C, Liu H Y, 1964. On specimens of *Metailurus* from Yushe, Shansi. Vert PalAsiat, 8: 182–186

Chang M J, Zhang C X, Ji X P et al., 2023. A new *Rattus* species and its associated micromammals from the Pliocene Yangyi Formation in Baoshan, western Yunnan, China. J Vert Paleont, 43: e2249063

Chang Z F, Zhang Y F, Li J L et al., 2014. The geological and geomorphic characteristic of late Quaternary activity of the Deqin-Zhongdian-Daju Fault. J Seismol Res, 37: 46–52

Chen G F, 2003. A new genus of Pliohyracinae (Hyracoidea, Mammalia) from the Late Pliocene of Dege, Sichuan, China. Vert PalAsiat, 41: 240–248

Chen G F, 2004. Order Artiodactyla. In: Zheng S H ed. Jianshi Hominid Site. Beijing: Science Press. 254–303

Chen G J, Wang W, Mo J Y et al., 2002. Pleistocene vertebrate fauna from Wuyun Cave of Tiandong County, Guangxi. Vert PalAsiat, 40: 42–51

Chen L, Song Y L, Xu S F, 2008. The boundary of palaearctic and oriental realms in western China. Prog Nat Sci, 18: 833–841

Chen X F, 1994. Stratigraphy and large mammals of the "Jinglean" Stage, Shanxi, China. Quat Sci, 14: 339–353

Chen Z Z, Pei X X, Song J L et al., 2023. Systematics and evolutionary history of the genus *Micromys* (Mammalia: Rodentia: Muridae). Mamm Biol, 103: 389–403

Cheng J, 1994. Discussion on the evolutionary history of Jinsha river from Benzilan to Jinjiangjie in northwestern Yunnan. J East China Geol Inst, 17: 234–241, 253

Chi H X, 1974. Late Pleistocene mammals from Lantian, Shensi. Vert PalAsiat, 12: 222–227

Chi H X, 1975. The Lower Pleistocene mammalian fossils of Lantian District, Shensi. Vert PalAsiat, 13: 169–177

Chia L P, Wang C, 1978. Hsihoutu–a Culture Site of Early Pleistocene in Shansi Province. Beijing: Wenwu Press. 1–85

Chow M C, Li C K, 1965. Mammalian fossils in association with the mandible of Lantian Man at Chen-Chia-Ou, in Lantian, Shensi. Vert PalAsiat, 9: 377–394

CSEQXP of CAS (The Comprehensive Scientific Expedition to the Qinghai-Xizang Plateau, the Chinese Academy of

Sciences), 1983. Studies in Qinghai-Xizang (Tibet) Plateau Special Issue of Hengduan Mountains Scientific Expedition (Book 1). Kunming: Yunnan People's Publishing House. 1–391

CSEQXP of CAS (The Comprehensive Scientific Expedition to the Qinghai-Xizang Plateau, the Chinese Academy of Sciences), 1986. Studies in Qinghai-Xizang (Tibet) Plateau Special Issue of Hengduan Mountains Scientific Expedition (Book 2). Beijing: Beijing Science & Technology Press. 1–623

Deng T, Xue X X, 1999. Chinese Fossil Horses of *Equus* and Their Environment. Beijing: China Ocean Press. 1–156

Denys C, Taylor P J, Aplin K P, 2017. Family Muridae (true mice and rats, gerbils and relatives). In: Wilson D E, Lacher T E, Mittermeier R A eds. Handbook of the Mammals of the World. Vol. 7. Rodents II. Barcelona: Lynx Edicions. 536–886

Ding W N, Ree R H, Spicer R A et al., 2020. Ancient orogenic and monsoon-driven assembly of the world's richest temperate alpine flora. Science, 369: 578–581

Dong W, 2006. Early Pleistocene Ruminants (Mammals) from the Dajushan, Huainan, Anhui Province (China). Vert PalAsiat, 44: 332–346

Dong W, 2008. Nouveau matériel de *Leptobos* (*Smertiobos*) *crassus* (Artiodactyla, Mammalia) du Pléistocène inférieur à Renzidong (Chine de l'Est). Geobios, 41: 355–364

Dong W, Fang Y S, 2004. The Cervidae (Artiodactyla, Mammalia) from the Tuozidong at Tangshan, Jiangsu Province, China. Acta Anthrop Sin, 23(Supp): 296–305

Dong W, Li Z Y, 2009. New cervids (Artiodactyla, Mammalia) from the Late Pleistocene of Lingjing site in Henan Province, China. Acta Anthrop Sin, 28: 319–326

Dong W, Qiu Z X, Wang F Z, 2009. Artiodactyla. In: Jin C Z, Liu J Y eds. Paleolithic Site – The Renzidong Cave, Fanchang, Anhui Province. Beijing: Science Press. 321–335

Dong W, Bai W P, Pan Y et al., 2020. New material of Cervidae (Artiodactyla, Mammalia) from Xinyaozi Ravine in Shanxi, North China. Vert PalAsiat, 58: 221–248

Du Y B, Wen Z X, Zhang J L et al., 2017. The roles of environment, space, and phylogeny in determining functional dispersion of rodents (Rodentia) in the Hengduan Mountains, China. Ecol Evol, 7: 10941–10951

Eisenmann V, Alberdi M T, de Giuli C et al., 1988. Studying Fossil Horses. Vol. I. Methodology. Leiden: E. J. Brill. 1–71

Erbajeva M A, 1988. Cenozoic *Pikas* (Taxonomy, Systematics, Phylogeny). Moscow: Nauka. 1–224

Erbajeva M A, Zheng S H, 2005. New data on Late Miocene-Pleistocene ochotonids (Ochotonidae, Lagomorpha) from North China. Acta Zool Crac, 48: 93–117

Fan Y B, Shao Q F, Bacon A M et al., 2022. Late Pleistocene large-bodied mammalian fauna from Mocun Cave in south China: palaeontological, chronological and biogeographical implications. Quat Sci Rev, 294: 107741

Forsyth Major C I, 1899. On fossil and recent Lagomorpha. Trans Linn Soc London, 2: 433–520

Gai P, Wei Q, 1977. The discovery of Upper Paleolithic Hutouliang Site. Vert PalAsiat, 15: 287–300

Gao F, Hou Y M, Li G et al., 2024. Brief report on Palaeolithic surveys of the western Xiaozhongdian plateau, Shangri-la, Yunnan Province. Quat Sci, 44: 442–452

Ge D Y, Feijo A, Wen Z X et al., 2021. Demographic history and genomic response to environmental changes in a rapid radiation of wild rats. Mol Biol Evol, 38: 1905–1923

Han D F, 1987. Artiodactyla fossils from Liucheng *Gigantopithecus* cave in Guangxi. Mem Inst Vert Palaeont Palaeoanthrop Acad Sin, 18: 135–208

Hao S D, Huang W B, 1998. Luobingdong Cave Site. Haikou: The South Press. 1–164

He K, Jiang X L, 2014. Sky islands of southwest China. I: an overview of phylogeographic patterns. Chinese Sci Bull, 59: 585–597

He S L, Ding L, Xiong Z Y et al., 2022. A distinctive Eocene Asian monsoon and modern biodiversity resulted from the rise of eastern Tibet. Sci Bull, 67: 2245–2258

Hou Y F, Zhang J, Cao Y P et al., 2022. Faunal remains of the Yangshao period from the Gouwan site, Xichuan County, Henan Province. Acta Anthrop Sin, 41: 913–926

Hu C K, Qi T, 1978. Gongwangling Pleistocene Mammalian Fauna of Lantian, Shaanxi. Palaeontol Sin, New Ser C, 21: 1–64

Huang J H, Huang J H, Lu X H et al., 2016. Diversity distribution patterns of Chinese endemic seed plant species and their implications for conservation planning. Sci Rep, 6: 33913

Huang W B, Fang Q R, 1991. Wushan Hominid Site. Beijing: Ocean Press. 1–230

Huang W B, Ji H X, 1963. Note on Holocene Hsienjen Cave deposit of Wannian, Kangsi. Vert PalAsiat, 7: 263–272

Jennings A P, Veron G, 2009. Family Viverridae (Civets, Genets and Oyans). In: Wilson D E, Mittermeier R A eds. Handbook of the Mammals of the World. Vol. 1. Carnivores. Barcelona: Lynx Edicions. 174–233

Ji H X (Chi H X), 1976. The Middle Pleistocene mammalian fossils of Laochihe, Lantian District, Shaanxi. Vert PalAsiat, 14: 59–66

Jiangzuo Q G, Zhang B, Deng L et al., 2018. Fossil Carnivora (Mammalia) from Yangjiawan Cave 2, Pingxiang, Jiangxi, with remarks about the tooth identification of Quaternary carnivores. In: Dong W ed. Proceedings of the Sixteenth Annual Meeting of the Chinese Society of Vertebrate Paleontology. Beijing: China Ocean Press. 119–146

Jin C Z, Liu J Y eds. 2009. Paleolithic Site–The Renzidong Cave, Fanchang, Anhui Province. Beijing: Science Press. 1–439

Jin C Z, Xu F, 2009. Lagomorpha. In: Jin C Z, Liu J Y eds. Paleolithic Site–The Renzidong Cave, Fanchang, Anhui Province. Beijing: Science Press. 162–165

Jin C Z, Zheng L T, Dong W et al., 2000. The Early Pleistocene deposits and mammalian fauna from Renzidong, Fanchang, Anhui Province, China. Acta Anthrop Sin, 19: 184–198

Jin C Z, Dong W, Gao X et al., 2004. Preliminary report on the 2002 excavation of Jinpendong site at Wuhu, Anhui Province. Acta Anthrop Sin, 23: 281–291

Jin C Z, Zhang Y Q, Wei G B et al., 2009a. Order Rodentia. In: Jin C Z, Liu J Y eds. Paleolithic Site – The Renzidong Cave, Fanchang, Anhui Province. Beijing: Science Press. 166–219

Jin C Z, Qin D G, Pan W S et al., 2009b. A newly discovered *Gigantopithecus* fauna from Sanhe Cave, Chongzuo, Guangxi, South China. Chinese Sci Bull, 54: 788–797

Jin C Z, Wang Y, Liu J Y et al., 2021. Late Cenozoic mammalian faunal evolution at the Jinyuan Cave site of Luotuo Hill, Dalian, Northeast China. Quat Int, 577: 15–28

Kostopoulos D S, Guy F, Kynigopoulou Z et al., 2018. A 2 Ma old baboon-like monkey from Northern Greece and new evidence to support the *Paradolichopithecus*-*Procynocephalus* synonymy (Primates: Cercopithecidae). J Hum Evol, 121: 178–192

Kurtén B, 1968. Pleistocene Mammals of Europe. New York: Weidenfeld and Nicolson. 1–326

Li C K, 2019. Family Leporidae. In: Li C K, Zhang Z Q eds. Palaeovertebrata Sinica. Vol. III. Beijing: Science Press. 50–96

Li Q, Ni X J, 2021. Wet sieving technique for collecting microfossils. Bio-protocol, 101: e1010613

Li T Y, Wang Z H, Li W S et al., 1994. Morphological features of human skulls from Quyuan River mouth, Yunxian, Hubei and their place in human evolution. Acta Anthrop Sin, 13: 104–192

Li Y, Ma X L, Cao Q et al., 2023. Response of an alpine plant to Quaternary climate change: a phylogeographic study of *Saxifraga tangutica* (Saxifragaceae) in the Qinghai-Tibetan Plateau and Himalayas. Braz J Bot, 46: 69–83

Li Y K, 2015. A mandible of *Leptobos* (Bovidae, Artiodactyla) from the Lower Pleistocene of Longdan, Gansu, China, and evidence of feline predatory strategy - addition to the Early Pleistocene Longdan Mammalian Fauna. Vert PalAsiat, 53: 193–205

Li Z F, Wang X L, Xu Y T et al., 2022. Changes of net primary productivity of vegetation from 1996 to 2015 in Shangri-La region. Acta Phytoecol Sin, 42: 266–276

Li Z J, Yu G H, Rao D Q et al., 2012. Phylogeography and demographic history of *Babina pleuraden* (Anura, Ranidae) in southwestern China. PLoS One, 7: e34013

Lin Y P, Pan Y R, Lu Q W, 1978. The mammalian fauna of Early Pleistocene from Yuanmou, Yunnan. In: Institute of Vertebrate Paleontology and Paleoanthropology, Chinese Academy of Sciences (IVPP) ed. Proceedings of Paleoanthropology of the Institute of Vertebrate Paleontology and Paleoanthropology. Beijing: Science Press. 101–125

Lin Y P, Pan Y R, Lu Q W, 1984. The Early Pleistocene fauna of Yuanmou Basin. In: Zhou G X, Zhang X Y eds. Yuanmou Man: A Collection of Photos and Eessays on Prehistoric Man and Cultures in Yuanmou Basin, Yunnan Province. Kunming: Yunnan People's Press. 141–162

Liu H Y, You Y Z, 1974. New materials of *Equus yunnanensis* in Yuanmou, Yunnan. Vert PalAsiat, 12: 126–136

Liu J N, Chang Y Q, Tian P et al., 2023. Geomorphic characteristics of drainage basins in Deqin-Weixi area and their response to tectonic activities. J Seismol Res, 46: 315–322

Liu J Y, Zhang Y Q, Chi Z Q et al., 2022. A Late Pliocene *Hipparion houfenense* fauna from Yegou, Nihewan Basin and its biostratigraphic significance. Vert PalAsiat, 60: 278–323

Liu L P, Zheng S H, 1997. Note on the Late Cenozoic lagomorphs of Danjiang Reservoir Area in Hubei and Henan. Vert PalAsiat, 35: 130–144

Liu L P, Galbrun E, Tang H et al., 2023. The emergence of modern zoogeographic regions in Asia examined through climate–dental trait association patterns. Nat Commun, 14: 8194

Liu S Z, Wang Y, Dong W et al., 2017. Preliminary report on the 2016's excavation at luotuoshan locality of Dalian, Liaoning Province. Quat Sci, 37: 908–915

López-Antoñanzas R, 2013. Dental morphology and wear pattern of bamboo rats, genus *Rhizomys* Gray, 1831 (Rodentia: Spalacidae). Zool Anz, 253: 85–92

Ma X P, Li G, Gao F et al., 2004. New Early Pleistocene mammalian materials from Zhongdian, Yunnan Province, China. Vert PalAsiat, 42: 246–258

Mao K S, Wang Y, Liu J Q, 2021. Evolutionary origin of species diversity on the Qinghai–Tibet Plateau. J Syst Evol, 59: 1142–1158

McKenna M C, Bell S K, 1997. Classification of Mammals Above the Species Level. New York: Columbia University Press. 1–631

Meng L H, Chen G, Li Z H et al., 2015. Refugial isolation and range expansions drive the genetic structure of *Oxyria sinensis* (Polygonaceae) in the Himalaya-Hengduan Mountain. Sci Rep, 5: 10396

Mittermeier R A, Gil P R, Hoffman M et al., 2005. Hotspots Revisited: Earth's Biologically Richest and Most Endangered

Terrestrial Ecoregions. Chicago: University of Chicago Press. 1–390

Mittermeier R A, Turner W R, Larsen F W et al., 2011. Chapter 1. Global biodiversity conservation: the critical role of hotspots. In: Zachos F E, Habel J C eds. Biodiversity Hotspots. Distribution and Protection of Conservation Priority Areas. Heidelberg: Springer-Verlag. 3–22

Myers N, Mittermeier R A, Mittermeier C G et al., 2000. Biodiversity hotspots for conservation priorities. Nature, 403: 853–858

Nanjing Museum and Institute of Archaeology, Jiangsu Province, 2007. The Early Pleistocene Mammalian Fauna at Tuozi Cave, Nanjing, China. Beijing: Science Press. 1–182

Norris R W, 2017. Family Spalacidae (muroid mole-rats). In: Wilson D E, Lacher T E, Mittermeier R A eds. Handbook of the Mammals of the World. Vol. 7. Rodents II. Barcelona: Lynx Edicions. 108–143

Norton C J, Jin C Z, Wang Y et al., 2010. Chapter 7: Rethinking the Palearctic-Oriental biogeographic boundary in Quaternary China. In: Norton C J, Braun D R eds. Asian Paleoanthropology: From Africa to China and Beyond. Vertebrate Paleobiology and Paleoanthropology. New York: Springer. 81–100

Pan Y, Zhang Y Q, Yang L Y et al., 2023. Preliminary description of a late Middle Pleistocene mammalian fauna prior to the extinction of *Gigantopithecus blacki* from the Yixiantian Cave, Guangxi ZAR, South China. Anat Rec, 308: 2730–2755

Patnaik R, 2001. Late Pliocene micromammals from Tatrot Formation (Upper Siwaliks) exposed near Village Saketi, Himachal Pradesh, India. Palaeontogr Abt A, 261: 55–81

Patnaik R, 2002. Pliocene Leporidae (Lagomorpha, Mammalia) from the Upper Siwaliks of India: implications for phylogenetic relationships. J Vert Paleont, 22: 443–452

Pei W C, 1940. Note on a collection of mammal fossils from Tanyang in Kiangsu Province. Bull Geol Soc China, 19: 379–392

Pei W C, 1961. Fossil mammals of Early Pleistocene age from Yuanmo (Ma-Kai) of Yunnan. Vert PalAsiat, 5: 16–30

Pei W C, 1987. Carnivora, Proboscidea, and Rodentia from Liucheng *Gigantopithecus* Cave and other caves in Guangxi. Mem Inst Vert Palaeont Palaeoanthrop Acad Sin, 18: 5–134

Pope G G, Brooks A S, Delson E, 2000. Asia, Eastern and Southern. In: Delson E, Tattersall I, Van Couvering J A et al. eds. Encyclopedia of Human Evolution and Prehistory. New York: Garland Publishing. 84–91

Qi G Q, 1985. Stratigraphic summarization of *Ramapithecus* fossil locality, Lufeng, Yunnan. Acta Anthrop Sin, 4: 55–69

Qiu Z D, 2020. Family Rhizomyidae. In: Qiu Z D, Li C K, Zheng S H eds. Palaeovertebrata Sinica. Vol. III. Beijing: Science Press. 296–307

Qiu Z D, Li Q, 2016. Neogene rodents from central Nei Mongol, China. Palaeontol Sin, New Ser C, 30: 1–684

Qiu Z D, Li C K, Hu S J, 1984. Late Pleistocene micromammal fauna of Sanjiacun, Kunming. Vert PalAsiat, 22: 281–293

Qiu Z X, 1987. Die Hyaeniden aus dem Ruscinium und Villafranchium Chinas. Münchner Geowiss Abh Reihe A, Geol Paläont, 9: 1–108

Qiu Z X, 2000. Nihewan fauna and Q/N boundary in China. Quat Sci, 20: 142–154

Qiu Z X, Deng T, Wang B Y, 2004. Early Pleistocene mammalian fauna from Longdan, Dongxiang, Gansu. Palaeontol Sin, New Ser C, 27: 1–194

Qiu Z X, Deng T, Wang B Y, 2009. First Ursine bear material from Dongxiang, Gansu - addition to the Longdan Mammalian

Fauna (2). Vert PalAsiat, 47: 245–264

Quintana J, Bover P, Alcover J A et al., 2010. Presence of *Hypolagus* Dice, 1917 (Mammalia, Lagomorpha) in the Neogene of the Balearic Islands (Western Mediterranean): description of *Hypolagus balearicus* nov. sp. Geobios, 43: 555–567

Schlosser M, 1924. Fossil primates from China. Palaeontol Sin, Ser C, 1: 1–16

Shou Z H, 1964. Economic Fauna of China-Mammals. Beijing: Science Press. 1–554

Smith A T, Xie Y, 2013. Mammals of China. Princeton: Princeton University Press. 1–400

Sun H, Zhang J W, Deng T et al., 2017. Origins and evolution of plant diversity in the Hengduan Mountains, China. Plant Diversity, 39: 161–166

Takai M, Maschenko E N, Nishimura T D et al., 2008. Phylogenetic relationships and biogeographic history of *Paradolichopithecus sushkini* Trofimov, 1977, a large-bodied cercopithecine monkey from the Pliocene of Eurasia. Quat Int, 179: 108–119

Tang Y J, Zong G F, Lei Y L et al., 1988. The Late Cenozoic and its Mammalian Fossils from Hanzhong Basin, Shaanxi. Beijing: Beijing Science and Technology Press. 1–47

Tapponnier P, Peltzer G, Le Dain A Y et al., 1982. Propagating extrusion tectonics in Asia: new insights from simple experiments with plasticine. Geology, 10: 611–616

Teilhard de Chardin P, 1938. The fossils from Locality 12 of Choukoutien. Palaeontol Sin, New Ser C, 5: 1–49

Teilhard de Chardin P, 1940. The fossils from Locality 18 near Peking. Palaeontol Sin, New Ser C, 9: 1–94

Teilhard de Chardin P, 1942. New Rodents of the Pliocene & Lower Pleistocene of North China. Pub Inst Géo-Biol, Pékin, 9: 1–101

Teilhard de Chardin P, Piveteau J, 1930. Les mammifères fossils de Nihowan (Chine). Ann Paléontol, 19: 1–134

Teilhard de Chardin P, Trassaert M, 1937. The Pliocene Cameliae, Giraffidae, and Cervidae of South Eastern Shansi. Palaeontol Sin, New Ser C, 1: 1–56

Teilhard de Chardin P, Young C C, 1931. Fossil Mammals from the Late Cenozoic of Northern China. Palaeontol Sin, Ser C, 9: 1–89

Tong H W, Shang H, Zhang S Q et al., 2006. Mammalian biostratigraphy of Tianyuan Cave, compared with that of Upper Cave at Zhoukoudian (Choukoutien). Acta Anthrop Sin, 25: 68–81

Tong H W, Hu N, Wang X M, 2012. New remains of *Canis chihliensis* (Mammalia, Carnivora) from Shanshenmiaozui, a lower Pleistocene site in Yangyuan, Hebei. Vert PalAsiat, 50: 335–360

Wang B Y, 2005. Beaver (Rodentia, Mammalia) fossils from Longdan, Gansu, China - Addition to the Early Pleistocene Longdan Mammalian Fauna (1). Vert PalAsiat, 43: 237–242

Wang B Y, Wu W Y, Qiu Z D, 2020. Family Cricetidae. In: Qiu Z D, Li C K, Zheng S H eds. Palaeovertebrata Sinica. Vol. III. Beijing: Science Press. 10–151

Wang H, 1988. An Early Pleistocene mammalian fauna from Dali, Shaanxi. Vert PalAsiat, 26: 59–72

Wang K L, Zhou X H, Liu D T et al., 2022. The uplift of the Hengduan Mountains contributed to the speciation of three *Rhododendron* species. Glob Ecol Conserv, 35: e02085

Wang W, Potts R, Yuan B Y et al., 2007. Sequence of mammalian fossils, including hominoid teeth, from the Bubing Basin caves, South China. J Hum Evol, 52: 370–379

Wang X Y, Liang D, Wang X M et al., 2022. Phylogenomics reveals the evolution, biogeography, and diversification history of voles in the Hengduan Mountains. Commun Biol, 5: 1124

Wang Y, Wang Y S, Wang Y D et al., 2021. The murid rodents associated with *Gigantopithecus* from Yanliang Cave of

Fusui, Guangxi, with discussion on stratigraphic sequence of the Pleistocene Murinae faunas from southern China. Acta Anthrop Sin, 40: 1041–1054

Wang Y S, Wang S T, Li Y S, 1999. Neotectonic characteristics of the Zhongdian-Lijiang region, Yunnan. J Chengdu Univ Technol, 26: 68–72

Wei F W, Yang Q S, Wu Y et al., 2022. Taxonomy and Distribution of Mammals in China. Beijing: Science Press. 1–622

White J A, 1991. North American Leporinae (Mammalia: Lagomorpha) from late Miocene (Clarendonian) to latest Pliocene (Blancan). J Vert Paleont, 11: 67–89

Wu W Y, 2020. Family Muridae. In: Qiu Z D, Li C K, Zheng S H et al. eds. Palaeovertebrata Sinica. Vol. III. Beijing: Science Press. 378–467

Wu W Y, Flynn L J, 2017a. The Lagomorphs (Ochotonidae, Leporidae) of Yushe Basin. In: Flynn L J, Wu W Y eds. Late Cenozoic Yushe Basin, Shanxi Province, China: Geology and Fossil Mammals. Vol. II. Small Mammal Fossils of Yushe Basin. Dordrecht: Springer. 31–58

Wu W Y, Flynn L J, 2017b. The Hamster of Yushe Basin. In: Flynn L J, Wu W Y eds. Late Cenozoic Yushe Basin, Shanxi Province, China: Geology and Fossil Mammals. Vol. II. Small Mammal Fossils of Yushe Basin. Dordrecht: Springer. 123–138

Wu W Y, Flynn L J, Qiu Z D, 2017. The Murine Rodents of Yushe Basin. In: Flynn L J, Wu W Y eds. Late Cenozoic Yushe Basin, Shanxi Province, China: Geology and Fossil Mammals, Vol. II. Small Mammal Fossils of Yushe Basin. Dordrecht: Springer. 179–198

Wu X Z, Zhou X M, Wang Y F, 2008. A preliminary report of the paleolithic site of Fulongguan from Yunxian, Hubei. Acta Anthrop Sin, 27: 33–37

Xing Y W, Ree R H, 2017. Uplift-driven diversification in the Hengduan Mountains, a temperate biodiversity hotspot. Proc Nat Acad Sci USA, 114: E3444–E3451

Xu C H, Han K X, Wang L H, 1974. The *Giantopithecus* fossils and associated fauna in Western Hubei. Vert PalAsiat, 12: 293–309

You Y Z, Qi G Q, 1973. New materials of Pleistocene mammals in Yuanmou, Yunnan. Vert PalAsiat, 11: 66–80

Young C C, 1927. Fossile Nagethiere aus Nord-China. Palaeontol Sin, Ser C, 5: 1–82

Young C C, Pei W C, 1933. On the fissure deposits of Chinghsinghsien with remarks on the Cenozoic geology of the same area. Bull Geol Soc China, 13: 63–71

Yu G, Zhang M, Rao D et al., 2013. Effect of Pleistocene climatic oscillations on the phylogeography and demography of red knobby newt (*Tylototriton shanjing*) from Southwestern China. PLoS One, 8: e56066

Zack S P, 2012. Deciduous dentition of *Didymictis* (Carnivoramorpha: Viverravidae): implications for the first appearance of "Creodonta". J Mamm, 93: 808–817

Zdansky O, 1924. Jungtertiäre Carnivoren Chinas. Palaeontol Sin, Ser C, 2: 1–149

Zdansky O, 1928. Die Säugetiere der Quartärfauna von Chou-K'ou–Tien. Palaeontol Sin, Ser C, 5: 1–146

Zhang D C, Boufford D E, Ree R H et al., 2009a. The 29°N latitudinal line: an important division in the Hengduan Mountains, a biodiversity hotspot in southwest China. Nord J Bot, 27: 405–412

Zhang D C, Zhang Y H, Boufford D E et al., 2009b. Elevational patterns of species richness and endemism for some important taxa in the Hengduan Mountains, southwestern China. Biodivers Conserv, 18: 699–716

Zhang X J, He K Z, Zhou Z G, 1996. Features of sporopollen assemblages and environment changes of Neogene in area of

western Yunnan. Geoscience, 10: 187–201

Zhang Y Q, 2017. Fossil Arvicolini of Yushe Basin: facts and problems of Arvicoline biochronology of North China. In: Flynn L J, Wu W Y eds. Late Cenozoic Yushe Basin, Shanxi Province, China: Geology and Fossil Mammals. Vol. II. Small Mammal Fossils of Yushe Basin. Dordrecht: Springer. 153–172

Zhang Z H, Zou B K, Zhang L K, 1980. The discovery of fossil mammals at Anping, Liaoning. Vert PalAsiat, 18: 154–162

Zhang Z H, Fu R Y, Chen B F et al., 1985. A preliminary report on the excavation of Paleolithic site at Xiaogushan of Haicheng, Liaoning Province. Acta Anthrop Sin, 4: 70–81

Zhang Z H, Liu J, Zhang H G et al., 1997. A Pleistocene mammalian fauna from Panxian Dadong, Guizhou Province. Acta Anthrop Sin, 16: 209–220

Zhang Z Q, 2019. Family Ochotonidae. In: Li C K, Zhang Z Q eds. Palaeovertebrata Sinica. Vol. III. Beijing: Science Press. 96–144

Zhao E, Yang D, 1997. Herpetological Fauna of the Hengduan Mountains. Beijing: Science Press. 1–303

Zhao X T, Zheng M P, Li D M, 2007. Formation and evolution of the ancient “Lake Xiaozhongdian” in Diqing, Yunnan and its relationship with development of the ancient “Lake Shigu” and the modern valley of the Jinsha River. Acta Geol Sin, 81: 1645–1651

Zheng L, Pan R L, Curnoe D, 2006. Fossil baboon found in Yunnan, China. Zool Res, 27: 635–636

Zheng S H, 1976. A Middle Pleistocene micromammals fauna in Heshui, Gansu, China. Vert PalAsiat, 14: 112–120

Zheng S H, 1983. Micromammals from the Hexian Man Locality. Vert PalAsiat, 21: 230–238

Zheng S H, 1984. Revised determination of the fossil Cricetine (Rodentia, Mammalia) of Choukoutien district. Vert PalAsiat, 22: 179–197

Zheng S H, 1993. Quaternary Rodents of Sichuan-Guizhou Area, China. Beijing: Science Press. 1–231

Zheng S H, 2004. Order Rodentia. In: Zheng S H ed. Jianshi Hominid Site. Beijing: Science Press. 1–410

Zheng S H, 2020. Family Arvicolidae. In: Qiu Z D, Li C K, Zheng S H et al. eds. Palaeovertebrata Sinica. Vol. III. Beijing: Science Press. 152–228

Zheng S H, Zhang Z Q, 2000. Late Miocene–Early Pleistocene micromammals from Wenwanggou of Lingtai, Gansu, China. Vert PalAsiat, 38: 58–71

Zheng S H, Zhang Z Q, 2001. Late Miocene-Early Pleistocene biostratigraphy of the Leijiahe Area, Lingtai, Gansu. Vert PalAsiat, 39: 215–228

Zheng S H, Wu W Y, Li Y et al., 1985a. Late Cenozoic mammalian faunas of Guide and Gonghe basins, Qinghai Province. Vert PalAsiat, 23: 89–134

Zheng S H, Yuan B Y, Gao F Q et al., 1985b. Fossil mammals with special evidence of the evolution of *Myospalax*. In: Liu T S ed. Loess and the Environment. Beijing: China Ocean Press. 67–72

Zong G F, 1987a. Note on some mammalian fossils from the Early Pleistocene of Di-Qing County, Yunnan. Vert PalAsiat, 25: 69–76

Zong G F, 1987b. Note on some mammalian fossils of Yanyuan, Sichuan. Vert PalAsiat, 25: 137–145

Zong G F, Jiang C, 1991. A preliminary observation on Carnivora from the Neogene locality of Yuanmou, Yunnan. Vert PalAsiat, 29: 136–142

Zong G F, Chen W Y, Huang X S et al., 1996. Cenozoic Mammals and Environment of Hengduan Mountains Region. Beijing: China Ocean Press. 1–279